# RESEARCH MEMORANDUM



## THE BASE PRESSURE AT SUPERSONIC SPEEDS ON TWO-DIMENSIONAL AIRFOILS AND BODIES OF REVOLUTION (WITH AND WITHOUT FINS) HAVING TURBULENT BOUNDARY LAYERS

By Eugene S. Love

Langley Aeronautical Laboratory
Langley Field, Va.



NATIONAL ADVISORY COMMITTEE
FOR AERONAUTICS

WASHINGTON

April 29, 1953

NATIONAL ADVISORY COMMITTEE FOR AERONAUTICS

RESEARCH MEMORANDUM

# THE BASE PRESSURE AT SUPERSONIC SPEEDS ON TWO-DIMENSIONAL AIRFOILS AND BODIES OF REVOLUTION (WITH AND WITHOUT FINS) HAVING TURBULENT BOUNDARY LAYERS

By Eugene S. Love

## SUMMARY

An analysis has been made of available experimental data to show the effects of most of the variables that are more predominant in determining base pressure at supersonic speeds. The analysis covers two-dimensional bases and the bases of bodies of revolution, with and without stabilizing fins, and is restricted to turbulent boundary layers. The present status of available experimental information is summarized as are the existing methods for predicting base pressure.

A simple semiempirical method that essentially extends the method of Cortright and Schroeder (NACA RM E51F26) is presented for estimating base pressure. For two-dimensional bases, this method stems from an analogy established between the base-pressure phenomena and the pressure rise required to separate the boundary layer. An analysis made for axially symmetric flow indicates that the base pressure for bodies of revolution is subject to the same analogy. Based upon the methods presented, estimations are made of such effects as Mach number, angle-of-attack, boattailing, fineness ratio, and fin effects. These estimations are shown to give fair predictions of experimental results.

## INTRODUCTION

The problem of predicting the base pressure at supersonic speeds has received considerable attention in recent years and several methods have been advanced recently (refs. 1 to 6), some of which give much more satisfactory results than the older methods (refs. 7 to 9). The work of Crocco and Lees (ref. 1) gives satisfactory qualitative predictions throughout the Reynolds number range and may ultimately give

satisfactory quantitative values if the problem of predicting the Reynolds number of transition in boundary layers and free wakes is sufficiently overcome and if some reliable basic end value of the base pressure can be used as a starting point in the calculations. The semiempirical method of Chapman (ref. 2 and additional comparisons in ref. 10) has proved satisfactory for the prediction of the base pressure on boattail bodies and airfoils when the boundary layer is turbulent. This method (ref. 2) utilizes experimental data on profiles without boattailing as compiled in reference 10. In reference 3, Cortright and Schroeder have presented a method for estimating the base pressure on a boattail body having a turbulent boundary layer that utilizes any data which provide the separation angle at the base as a function of Mach number ahead of the base. Existing comparisons between this method and that of reference 2 appear to indicate that both methods give, in general, reasonable agreement with experimental measurements of boattail effects for bodies of revolution and for two-dimensional airfoils. The method of Cope (ref. 5) does not appear to give as satisfactory a prediction as that of Chapman and, as Cope has pointed out, the approximations and assumptions involved result in a first approximation only. Little is known by the present author of the recent method of Gabeaud beyond the information given in reference 4; therefore, the limits of its applicability are unknown. Gabeaud does appear to confine his comparisons to experimental data from finned bodies of revolution, but since the equation as given in reference 4 includes no terms to cover fin effects, the value of the method remains in question. The method of Kurzweg (ref. 6) appears inadequate since it gives identical results for airfoils and bodies of revolution.

To date, considerable experimental work has been devoted to investigations of base pressure at supersonic speeds. The reported investigations are too numerous to make reference to all herein, but references 11 to 33, in addition to certain of those previously mentioned, are examples of work that has been done to determine the effects of various variables upon base pressure. References 2, 18, 19, 22, and 27 report investigations in which the effects of support interference upon base pressure have been studied. References 2 and 18 include investigations of the effects of disturbances entering the wake (ref. 2 with sting support, and ref. 18 without sting support). A number of the references show the variation of base pressure with Reynolds number at a constant Mach number. (See refs. 2, 6, 11, 17, 18, 27, 31, and 32, for example.) These and other references show the effects for bodies of revolution of such influencing variables as the presence of fins, location of fins, jet flow, nose and base shape, and boattail angle. Reference 12 and parts of references 29 and 33 are examples of studies devoted to essentially two-dimensional base pressures. With this accumulation of experimental data and the compilations of data now in existence, particularly those in references 2 and 10, ready assessment may be made of the effects of most of the primary influencing variables

as well as an evaluation of any method advanced to predict these effects. However, as will be shown, there is still a need for experimental information on the effects of certain variables, particularly those associated with fin effects on bodies of revolution.

In the present investigation, only bodies and wings having turbulent boundary layers ahead of their bases are considered. This restriction to turbulent boundary layers is not severe for practical application since, at the Reynolds numbers for full-scale aircraft or missiles, the likelihood of realizing complete laminar flow over the body or wing is remote, particularly so for the body; in addition, the presence of stabilizing fins causes transition even at low Reynolds numbers. (See ref. 18.) The advantage of this restriction is that it permits effects of Reynolds number to be ignored. References 2, 10, 12, 15, and 31, for example, have shown that, once a fully turbulent boundary layer exists ahead of the base, the variation in base pressure with increasing Reynolds number is small.

The purpose of this investigation is to make a summary analysis of available experimental data, including some results obtained recently in the Langley 9-inch supersonic tunnel, to show the effects of most of the variables that are more predominant in influencing base pressure and to advance, where possible, simple semiempirical methods for the prediction of these effects. These methods, while they may not be significantly advantageous over or much different from methods now in existence, are believed to show a more direct relation between wake and body geometry. Furthermore, a viscous analogy is established between the trailing shock and the pressure rise required to separate the boundary layer. The first portion of this paper will deal with two-dimensional base pressures. The second portion will deal with the base pressure on bodies of revolution and will be covered in two sections: bodies without fins and bodies with fins.

## SYMBOLS

| | |
|---|---|
| $\alpha$ | angle of attack |
| $M_\infty$ | free-stream Mach number |
| $M_0$ | Mach number ahead of base |
| $M_1$ | Mach number ahead of trailing shock |
| $p_1$ | static pressure ahead of trailing shock |
| $q_1$ | dynamic pressure ahead of trailing shock |

$p_2$ static pressure behind trailing shock

$P_r$ pressure-rise coefficient required to separate a boundary layer, $\frac{p_2 - p_1}{q_1}$

$\delta$ the critical angle for a two-dimensional turning of the flow through a shock that will cause the boundary layer to separate

$P$ pressure coefficient, $\frac{p_l - p_\infty}{q_\infty}$

$P_B$ base pressure coefficient, $\frac{p_B - p_\infty}{q_\infty}$

$p_B$ base pressure

$p_l$ local pressure

$p_\infty$ free-stream static pressure

$q_\infty$ free-stream dynamic pressure

$\beta$ boattail angle

$\theta$ angle between free-stream direction and the edge of the converging wake in axially symmetric flow

$\eta$ local inclination of body surface with respect to body center line

$\delta_e$ effective two-dimensional expansion angle at base of bodies of revolution

$D$ maximum body diameter

$h$ base diameter

$t$ fin thickness

$c$ fin chord

$t_w$ wake thickness just behind trailing shock

$x$ distance from trailing edge of fin to base of body (positive when trailing edge is ahead of base) measured parallel to body center line

| | |
|---|---|
| N | distance between base of body and approximate location of base of trailing shock, measured parallel to body center line |
| L | body length |
| R | Reynolds number |
| y | distance from body center line measured normal to body center line |
| $\varphi$ | angle between meridian of fin and any other meridian |
| $\gamma$ | ratio of specific heats for air |

## I - TWO-DIMENSIONAL BASE PRESSURE

Analogy to pressure rise for separation of boundary layer.- The recent compilation of data reported in reference 34 has shown the pressure rise across a shock wave that is necessary to cause separation of the boundary layer on a flat plate with a forward-facing step. In that investigation, the Prandtl pressure-rise coefficient (see ref. 35) is presented in terms of the ratio of the difference between the static pressures behind and ahead of the shock to the dynamic pressure ahead of the shock. The data compiled in reference 34 and recent results obtained in the Langley 9-inch supersonic tunnel (9 in. SST) and the mixing-zone apparatus (MZA) of the Langley 9-inch supersonic tunnel are shown in figure 1. Of the indicated variations of $P_r$ with R, the greatest appears to be proportional to $R^{-1/12}$ which is considerably less than the theoretical variation proportional to $R^{-1/5}$. The least variation is essentially zero. Examination of these data and their sources indicated that, within the accuracy of the test procedures employed, the pressure-rise coefficient experiences small or almost no variation with Reynolds number when the boundary layer is turbulent provided the step height (fig. 2(a)) is at least several times the boundary-layer thickness. For the purposes of the present investigation, this variation is assumed to be negligible since it is of the same order as the variation of base pressure with Reynolds number when the boundary layer is turbulent.

Figure 2(a) gives a sketch of the separation phenomena on a flat plate. Since the supported boundary layer (boundary layer adjacent to a surface) will withstand only a certain critical value of $P_r$ before separating, there seems little reason to believe that an unsupported boundary layer (free wake) would have a critical value of $P_r$ that is much different. This critical condition for separation may be expressed

in terms that are more analagous to the physical characteristics of the flow behind a two-dimensional base: that is, the angle through which the flow is turned has a critical value $\delta$ for a given value of $M_1$ that cannot be exceeded. Comparison of figures 2(a) and 2(b) shows the analogy between the separation phenomena and the flow behind the base. On the basis of this analogy, the experimental values of $P_r$ as a function of $M_1$ may be used to obtain the static pressure ratio $p_2/p_1$ across the shock and, thereby, the value of $\delta$ may be calculated. Once $\delta$ is known, $M_o$ is determined, and the variation of the base pressure coefficient $P_B$ with $M_o$ may be computed from the variation of $M_1$ with $M_o$. Figure 3 presents the variation of $P_r$ with $M_1$. Each point represents the value of $P_r$ averaged over the Reynolds number range for the particular value of $M_1$. The values of $M_1$ were selected on the basis of the examination of the data described in the previous paragraph. With the exclusion of the point at $M_1 = 3.03$, all data were flat-plate data. The data for $M_1 = 3.03$ were obtained by sliding two circular collars along a tube having a radius of 1.47 inches. The ratio of the radius of the collar to the radius of the tube was approximately 1.2 for the larger collar and 1.1 for the smaller collar. Accordingly an approximation of the three-dimensional effect was made and applied as a correction to the point at $M_1 = 3.03$ as indicated in figure 3. This correction was obtained by measuring the angle of flow deflection along the boundary of the separated region close to the beginning of separation.

The calculated variation of $\delta$ with $M_o$, based upon the curve through the experimental values of $P_r$ and the extrapolation beyond $M_1 = 3.03$, is shown by the lower curve in figure 4. The corresponding base pressures are shown by the solid line in figure 5. Also shown in figure 5 are the curves of absolute limiting base pressure (vacuum), inviscid limiting base pressure (maximum-deflection trailing shock), and the experimental data compilations from references 10 and 29. The predicted magnitude and variation of base pressure with Mach number calculated from the pressure rise necessary to separate the boundary layer is seen to be in fair agreement with the experimental results. The fact that the predicted base pressure is slightly higher than experiment may be due to several factors: first, the effects of a small variation of $P_r$ with R; second, the predicted values correspond to isentropic flow ahead of the base; third, the mixing profile might be altered over the free jet region by the presence of vorticity in the "semidead air" region in a manner which would increase the maximum $P_r$; and fourth, the free wake may withstand a higher $P_r$ as the result of the absence of the damping effect upon turbulent oscillations within the boundary layer that is created by the presence of a solid surface. An increment of 0.06 added to $P_r$ as shown by the

upper curve in figure 3 gives the upper curve of $\delta$ against $M_o$ in figure 4 and the slightly lower base pressures shown in figure 5.

In reference 36, some results are given for the pressure rise across the trailing shock behind a rearward-facing step as Mach number and the slope of the surface following the step are varied. Through the experimental range of $M_1$ from about 1.8 to 3.4 the results are shown to be in good agreement with the empirical relation

$$\frac{p_2 - p_1}{p_1} = \frac{M_1^2}{4} \tag{1}$$

In terms of the previously defined pressure-rise coefficient, equation (1) gives the interesting result that $P_r$ is independent of $M_1$ and is equal to $1/2\gamma$. The curve showing the variation of $P_B$ with $M_\infty$ calculated from this constant value of $P_r$ has been entered on figure 5 for comparison. As would be expected, the predicted values of $P_B$ tend to be high at the lower Mach numbers and low at the higher Mach numbers. The results from the forward-facing steps are, therefore, more reliable for predicting base pressure than the results from the rearward-facing step with varying slope of the afterbody surface. This would seem to indicate that the establishment of the position of the shock is more analogous to the conditions of the trailing shock common to base phenomena when the turning of the flow is created by a separated region rather than by a solid surface.

Effects of boattailing.- The variation of $\delta$ with $M_o$ given in figure 4 may be used to calculate the effects of boattailing on two-dimensional airfoils where $\beta \leq \delta$. Since $\delta$ is measured with respect to free-stream direction and defines the limiting turning angle of the flow through the trailing shock, the value of boattail angle $\beta$ is subtracted from the value of $\delta$ that corresponds to the Mach number immediately ahead of the base to obtain the value of $\delta$ to be used in computing the base pressure. (This procedure is the same as that of Cortright and Schroeder presented in ref. 3.)

When $\beta$ exceeds $\delta$ the base phenomena is complicated by the fact that the expansion which existed at the corner of the base is replaced by a compression, or shock, The base phenomena thus includes two shocks whose strengths are interrelated. For a given configuration the shock at the corner of the base may be related to the necessary conditions of the trailing shock (based upon $P_r$ as before) through the usual two-dimensional shock relations. So long as the pressure rise across the shock from the corner of the base does not reach $P_r$,

this shock will remain at the corner. However, when $\beta$ becomes sufficiently large, $P_r$ will have been exceeded and the shock at the corner will move forward onto the boattail or body surface until a point of equilibrium is reached for which the pressure rise is equal to $P_r$. For boattails formed by flat surfaces and having an abrupt beginning, such as a shoulder, the shock at the corner will move rapidly, if not immediately, from the corner to the shoulder when $P_r$ for this shock is exceeded. Consequently, at very large $\beta$ this shock would disappear for such boattail shapes since at $\beta = 90^\circ$ all conditions are, within the assumptions, identical to those for $\beta = 0^\circ$. The base pressure at large boattail angles must, therefore, tend to revert to the value at $\beta = 0^\circ$.

In all calculations by the present method, the pressure and Mach number ahead of the base are taken into account. When separation occurs on the boattail the Mach number and pressure ahead of the separation point are used as described in the preceding paragraph.

In figure 6, predictions of the effects of boattailing by the present approach are compared with experimental results and the estimates of Chapman as given in reference 10. No estimate is shown for the method of Cortright and Schroeder since when applied to the results of figure 4 it gives an estimate through $\beta \leq \delta$ that is identical with the present estimate. The basic (lower) curve of figure 4 has been used in the calculations for the present estimate and the calculated curve of base pressure has, with one exception, been shifted to pass through the value at $\beta = 0$, when necessary, to agree with the initial condition of Chapman's estimate. The same procedure has been used for the curves in figure 7 where comparison is made of the present estimate and results obtained in reference 29. In the comparisons of figure 6 at $M_\infty = 1.50$, the lack of experimental results at $\beta = 0$ prevents any reliable assessment of the methods. However, the value for $\beta = 0$ is believed to be somewhat lower than that assumed in reference 10, since for large boattail angles the value of $P_B$ must be approximately equal to that for $\beta = 0^\circ$. For this reason, and on the basis of results to be presented in figure 7 at $M_\infty = 1.41$, the present estimate has been faired as shown. The comparisons at $M_\infty = 2.00$ in figure 6 seem to indicate that the present estimate indicates trends that tend to follow the experimental results.

In figure 7 the present estimate shows fair agreement with the experimental variation. The fact that the base pressure does decrease noticeably with increasing boattail angle at $M_\infty = 1.41$ and slightly at $M_\infty = 1.62$ would appear to justify the value of $\beta = 0$ assumed for the present estimate at $M_\infty = 1.50$ in figure 6. The results of figure 7 indicate that the present method of estimation will give a fair prediction of effects of boattailing. Both the method and the experimental

results show that in the lower range of $\beta$ increasing the boattail angle will decrease the base pressure below $M_0 \approx 1.9$ and will increase the base pressure beyond $M_0 \approx 1.9$. The estimate of Chapman has not been included in figure 7 since it gives almost zero variation from the value at $\beta = 0$. Some of the erratic variation in the experimental values shown in figures 6 and 7 may be due to the fact that the base heights are of the same order as the thickness of the boundary layer, an unavoidable condition for thin airfoils with boattailing.

Factors other than those accounted for in the estimations by the present method can affect the reversion of the base pressure at large $\beta$ toward the value for $\beta = 0^\circ$. The circulation within the wake and the thickening of the turbulent wake boundaries as they approach juncture would, for values of $\beta$ where separation has occurred on the boattail surface, permit back-pressure effects from the trailing shock to be important. Back-pressure effects would (for a given $\beta$) also be related to the ratio of base height to maximum height. For ratios near zero it is obvious that the base-pressure reversion must be gradual since the base is moving slowly away from a position of close proximity to the base of the trailing shock whose back-pressure effects would tend to make the base pressure high. For ratios near 1.0 these effects would be negligible since the base is never in close proximity to the base of the trailing shock.

Angle-of-attack effects.- In references 10 and 12, the effect of angle of attack for two-dimensional bases with and without boattailing has been shown to be small, if not negligible, for $M_\infty = 1.5$ to 4 and for angles of attack up to $9^\circ$. Additional results that have been obtained in the Langley 9-inch supersonic tunnel are shown in figures 8 to 12 (fig. 11(b) excluded) and include some minor examples of the effects of Reynolds number which, although they are not within the proposed scope of this paper, have been included to show the conditions for which the boundary layer was turbulent ahead of the base. The model configuration, which spanned the test section of the tunnel, is shown at the top of figure 8. In all tests the vertical distribution of pressure across the base of the model at the midspan station was measured and found to be essentially constant at all angles of attack and at all Reynolds numbers. Examples of this distribution will be presented subsequently.

The data of figure 8 show that with a turbulent boundary layer the variation in $P_B$ with $\alpha$ is small and that once $\alpha$ reaches a value sufficient to cause a compression at the base corner of the upper surface, further increase in $\alpha$ increases the base pressure. Estimation of the variation in $P_B$ with $\alpha$ by the present method was made at $M_\infty = 2.41$ and, as shown in figure 8(d), the estimation is in good agreement with the experimental results. (The estimated curve has been

shifted slightly to allow the value at $\beta = 0$ to be in general agreement with the experimental values.)

Figure 9 presents some observations of the phenomena at $M_\infty = 1.93$. An example of the vortex street which forms in the wake behind the trailing shock (reported in more detail in ref. 12) is shown in figure 9(a). Figure 10 presents additional observations of the base phenomena at $M_\infty = 2.41$ for various angles of attack and Reynolds numbers. All the photographs show the presence of the lip shocks that extend rearward from the corners of the base; these shocks arise from the tendency of the flow to overexpand initially as it turns the corner, so that a shock is required to turn the flow in the direction determined by the mixing boundaries of the so-called dead-air region as shown in figure 11(a). The inclination of the mixing boundaries and the lip shocks are, therefore, directly related, and as shown in figure 12, their inclinations vary with Reynolds number until a fully turbulent boundary layer exists ahead of the base. (While two-dimensional bases facilitate the observation of these weak lip shocks, it is of interest to note that lip shocks have been observed in the flow about the base of a body of revolution. An example of this is shown in figure 11(b) which presents a photograph obtained in tests of a $15^\circ$ cone-cylinder in a ballistic range in the Langley gas dynamics laboratory. In axially symmetric flow the lip shocks are seen to be curved.) No attempt is made to account for the presence of these weak shocks in the estimates of base pressure in this report.

On the basis of the configuration employed and the results shown in figure 8, an analogy may be drawn for the base separating two supersonic streams having different Mach numbers and different static pressures just ahead of the base but essentially equal stagnation pressures. (For example, at $M_\infty = 2.41$ and $\alpha = 20^\circ$, $M_0 \approx 3.40$ on the upper surface and 1.58 on the lower surface.) If the particular values of the Mach numbers and static pressures on either side of a base are such that they can be resolved to essentially the same Mach number and static pressure by superimposing angle of attack, then the base pressure may be estimated by the present method.

General remarks.- In view of the reasonably close analogy that has been shown to exist between two-dimensional base pressures and the pressure rise through a shock required to separate the boundary layer from a flat plate, the reverse of the procedure may obviously be applied; that is, measurements of base pressures may be accepted as a means of estimating the pressure rise for separation of the boundary layer. Investigation of this analogy for laminar boundary layers and laminar wakes might, with the additional consideration of Reynolds number, lead to an establishment of the Reynolds number for wake transition and thereby supply one of the critical values for the prediction of base pressure with laminar boundary layers. On the basis of

existing experimental results and analyses, it appears permissible to assume for engineering estimates that the base pressure on two-dimensional bodies will be unaffected by boattail angle or angle of attack.

## II - BASE PRESSURE ON BODIES OF REVOLUTION

### Bodies Without Fins

Analogy to pressure rise for separation of the boundary layer.- For bodies of revolution, and therefore for axially symmetric flow, the quantitative analogy between the pressure rise required to separate the boundary layer and the base pressure is not readily established; however, accepting the idea that the pressure rise required to separate the boundary layer determines the base pressure permits a qualitative analogy to be drawn.

Figure 13 presents a sketch of the flow phenomena at the base of a body of revolution for which the variation in Mach number on the body surface is zero. The converging wake (A to B) is essentially conical and must experience a recompression along AB, whereas for two-dimensional flow the convergence of the wake would cause no change in pressure from that corresponding to the completed expansion at A. For the body of revolution, therefore, there is a decrease in Mach number along AB such that immediately ahead of B the local Mach number is considerably less than would be the case for a two-dimensional base with the same value of Mach number at A. Exactly at B the turning of the flow may be considered two dimensional; consequently, the two-dimensional pressure-rise coefficient would apply exactly at B and the value of $M_1$ would be that immediately ahead of B. It becomes obvious, therefore, that in order to realize the same value of $M_1$ just ahead of the base of the trailing shock for a two-dimensional base and the base of a body of revolution, each having the same degree of wake convergence, the value of the Mach number ahead of the base $M_0$ must be considerably greater for the body of revolution. From the above reasoning and in view of the variation of $\delta$ with $M_0$ shown in figure 4, the base pressure on bodies of revolution would be expected to be considerably higher than that on two-dimensional bodies at low and moderate supersonic speeds and equal to or slightly less than that on two-dimensional bodies at high supersonic speeds.

Although experimental base-pressure results tend to confirm the preceding qualitative analysis, quantitative confirmation through calculations based on $P_r$ is desirable; however, it would be necessary to know the distance N (see fig. 13) before any reverse calculation could be made of the Mach number variation from B to A. This distance would of necessity have to be measured from experimental results and the location of the point B would be subject to considerable error.

For this reason and from consideration of the inherent errors involved in a reverse calculation of this type (method of characteristics), no attempt has been made to apply this approach. Instead, measurements have been made, from published schlieren photographs and shadowgraphs, of the angle $\theta$ (see fig. 13) between free-stream direction and the clearly defined outer boundary of the convergent wake. The main part of these measurements was obtained from shadowgraphs made by The Ballistic Research Laboratories (BRL), Aberdeen Proving Ground, examples of which are shown in reference 2. The results are shown in figure 14.

Several values of $\theta$ and $M_o$ from figure 14 were utilized in attempts to calculate the Mach number variation along the surface of a cone replacing the convergent wake to determine whether a reasonable approximation of the required value of $M_1$ could be obtained at some station ahead of the tip of the cone. The method of characteristics was used first in these calculations. All the results showed that, if reliable pressures were to be obtained over the rear portion of the cone, more and more points must be added to the characteristic net as the cone tip is approached. Because of this complication, the calculations were confined to $M_o = 2.00$ and $\theta = 10.33^\circ$; the results are shown in figure 15. The third refinement to the calculations, which gave 44 points along the cone surface, gave a value of $M_1$ of approximately 1.60 at the cone tip as compared to the critical value of about 1.58 determined from $P_r$. It is difficult to estimate whether further refinements to the characteristic calculations would lower the calculated value of $M_1$ much further, but the fact that the value thus calculated and that determined from $P_r$ are of the same order would seem to offer, at least, support for the qualitative analogy presented previously. The less exact method of small disturbances was used in several 30-point calculations and, excluding the rearward 5 to 10 percent of the cone where the predicted values begin to increase rapidly toward infinite pressure at the tip, these results also gave values of $M_1$ of the same order as those determined from $P_r$. Furthermore, the results of reference 18 would appear to indicate that the theoretically predicted positive pressures over the rear of a parabolic convergent afterbody are realized experimentally.

Recently, measurements have been made in the Langley 9-inch supersonic tunnel of the recompression along the surface of a $10^\circ$ conical afterbody preceded by a cylindrical section and within the wake behind the base of a cylindrical semibody of revolution mounted on a boundary-layer-removal plate. The results for the $10^\circ$ conical afterbody are presented in figure 16 and show clearly that the recompression along the cone surface reaches positive values and is of the order of magnitude predicted theoretically. Figure 17 presents the wake pressures measured on the surface of the boundary-layer plate for which orifices

were located along an extension of the body center line and along a $10^{\circ}$ ray passing through the shoulder of the base. Although the wake pressures thus measured are subject to the effects of the presence of the plate surface, they are believed to represent a reasonably accurate picture of the true variation of the wake pressures with the possible exception of regions very close to the base. At $M = 1.93$ a direct comparison may be made between the results of figures 16 and 17 since, as shown in figure 14, the value of $\theta$ at $M = 1.93$ is very close to $10^{\circ}$. Such a comparison shows that the recompression along the wake boundary is very similar to that on the conical afterbody and that the recompression tends to be slightly greater for the wake boundary; thus, the calculated recompression at $M_0 = 2.00$ presented previously would appear to be a conservative estimate. These results coupled with the preceding analysis tend to substantiate the idea that the pressure rise required to separate the boundary layer is the predominant factor in determining the base pressure in axially symmetric as well as two-dimensional flow.

The results of figure 17 appear to be of additional significance in that the results at all Mach numbers show that the general assumption of constant pressure within the convergent wake behind a body of revolution is not permissible.

Simplified relation to wake convergence.- The upper curve of figure 14 through a Mach number of about 4, is faired through the measured experimental values of wake convergence $\theta$ presented as a function of the Mach number ahead of the base. The double symbol for a given measurement represents the limits of measurement of $\theta$ from both sides of the wake. All experimental points represent the case of zero boattailing, and no measurements were made for bodies having fineness ratios less than 5. If the cylindrical afterbody was not sufficiently long to allow the assumption that the Mach number ahead of the base was close to free-stream Mach number, the Mach number ahead of the base was determined by the method of characteristics. Figure 18 presents a compilation of experimental base-pressure data for bodies of revolution with cylindrical afterbodies (zero boattailing) including a curve representing the compilation of experimental data by Chapman from reference 10. For several of the experimental values of base pressure in the Mach number range from 1 to 4, the effective two-dimensional expansion angle $\delta_e$ at the base was calculated and compared with the values of the measured axially symmetric expansion angle $\theta$. In all instances $\delta_e$ was approximately 85 percent of $\theta$. Because of the recompression that exists from A to B (see fig. 13) and the influence of this recompression on the base pressure, $\theta$ would be expected to be somewhat larger than $\delta_e$. From $M_0 = 1$ to 4 the curve of $\delta_e$ in figure 14 was determined as 85 percent of the curve of $\theta$. Beyond $M_0 = 4$, the values of $\delta_e$ were computed from the experimental values of base

pressure from figure 18 and the curve of $\theta$ in figure 14 was faired as shown by assuming the 85-percent factor to hold throughout the Mach number range. It is interesting to note that, within experimental accuracy, the maximum value of $\theta$ is equal to the maximum value of $\delta$ given by the basic curve of figure 4. The fact that this equality exists lends further weight to the analogy that has been presented, since it must exist if the basis for the analogy is correct.

The curve of base pressure coefficient $P_B$ plotted against $M_o$ represented by the variation of $\delta_e = 0.85\theta$ against $M_o$ is entered on figure 18. For comparison with the experimental results, curves of the absolute limiting base pressure (vacuum) and the prediction of Gabeaud (latest method, ref. 4) have been included. Beyond $M_\infty = 3$ the prediction of Gabeaud is seen to give a good estimate of the experimental results. However, as stated previously, little is known of the method except the meager information of reference 4. All available information indicates that Gabeaud confines comparisons with his method to finned bodies of revolution. Agreement of the method with results from finned bodies, particularly at Mach numbers below about 3 must, as in reference 37, be considered fortuitous since the relation given in reference 4 includes no terms to cover fin effects. As will be shown later, these effects result from combinations of several variables and are significant. The only conclusion that will be drawn here is that the method of Gabeaud is satisfactory for bodies of revolution (no fins) with turbulent boundary layers and zero boattailing for $M_\infty = 3$ or greater. Whether this method is intended to be applicable to these conditions is not known.

Effect of fineness ratio of cylindrical afterbody.- In the preceding discussion, the relation between $P_B$ and $\delta_e$ was established for the Mach number ahead of the base on bodies having fineness ratios of 5 or greater. The fineness ratio of the cylindrical afterbody for these bodies was always 3 or greater. For shorter cylindrical afterbodies the variation of the pressure along the surface of the body from the point of juncture of the nose shape and the cylindrical section to the base can be appreciable and is a function of nose shape and Mach number. As the afterbody length is varied, the Mach number and pressure immediately ahead of the base vary and the base pressure would be expected to vary accordingly. Additional effects upon the base pressure may result from the pressure field (created by the nose shape) acting upon the wake boundaries but no attempt will be made to account for these effects. In this approximation, therefore, the prediction of $P_B$ as fineness ratio $L/h$ (or $L/D$) is varied becomes simply a calculation of the pressure and Mach number immediately ahead of the base and the application of the value of $\delta_e$ from the curve in figure 14. In this and other discussions to follow, the pressure and Mach number ahead of the base have been calculated by the method of characteristics, unless otherwise stated.

Figure 19 presents results of base-pressure measurements made in the Langley 9-inch supersonic tunnel on cone-cylinder bodies with varying afterbody length. The semiapex angle of the cone was $15^{\circ}$ and a transition strip was located 1/2 inch ahead of the shoulder. As shown, the effect of varying Reynolds number was small. At all Mach numbers the method employed gives a reasonable prediction of the effect of afterbody length on the base pressure. The slightly higher experimental base pressures, as compared with the estimates, may be attributed to the neglect of the effects of the body-induced pressure field upon the wake boundaries and to the use of artificial transition which has been shown in several investigations to cause the base pressure to be 5 to 10 percent higher than that for natural transition. (See ref. 27, for example.) While the correlation factor $(L/h)R^{-1/5}$ proposed in reference 2 seems more than justified for a configuration where variations in $L/h$ have small effect upon the pressure and Mach number ahead of the base, and in such applications is supported by the work of Crocco and Lees (ref. 1), the results shown in figure 19 indicate that application of this factor to bodies having appreciable variation in $M_o$ and $p_o$ with $L/h$ would be questionable. It is obvious that $L/h$ is by far the predominant factor in determining base pressure for such bodies. The results for cone-cylinder bodies correlated in reference 2 in terms of $(L/h)R^{-1/5}$ show a correlation curve that because of the small range of $R$ resembles the curve which would result from an $L/h$ variation only. If a particular value of $L/h$ were assumed to have a large range of $R$ in comparison to other values of $L/h$, it becomes apparent that a calculation of base pressure from the correlation curve for this particular $L/h$ would be subject to significant error. The results of reference 27 over a narrow range of $R$ show that other inadequacies exist in this form of correlation for bodies having varying $M_o$ and $p_o$ with $L/h$.

Figure 20 presents reproductions of shadowgraphs obtained in an investigation at the Ballistic Research Laboratories, Aberdeen Proving Ground, reported in reference 21. The models were cone-cylinders having varying afterbody lengths as shown and semiapex angles of approximately $10^{\circ}$. Free-stream Mach number was about 1.84. The Mach number ahead of the base $M_o$ is indicated for each model. (The value of $M_o$ for the cone corresponds to a vanishingly short afterbody.) Entered on the shadowgraphs are the tangents to the wake boundaries that were used to measure $\theta$, as are the particular values of $\theta$. The general agreement between these values of $\theta$ with the values given by the curve of figure 14 at the corresponding Mach numbers ahead of the base tends to give further indication that the effect of varying afterbody length upon base pressure is essentially the results of the variation in Mach number and pressure ahead of the base.

In figure 21 the compilation of experimental data by Chapman (ref. 2) for a cone-cylinder of $\frac{L}{h} = 5$ and the calculations by Chapman based upon wake measurements are compared with the present method for predicting the effect of afterbody length. Also included for comparison is the curve representing the condition for $M_0 = M_\infty$ as given in figure 18. The present method gives a good prediction throughout the range of experimental data with the exception of the lowest Mach numbers. In this vicinity, however, the nose shock is approaching detachment and the resulting variations in entropy and, possibly more important, the variations in base pressure due to transonic effects would be expected to cause significant deviations of experiment from either of the methods. The estimated variations of figure 21 also indicate that the effect of shortening the afterbody decreases with increasing Mach number.

Effects of boattailing.- In the section on two-dimensional base pressures, the effect of boattailing when $\beta \leq \delta$ was shown to be reasonably estimated by subtracting $\beta$ from $\delta$. For axially symmetric flow, however, the application of the same method (i.e. $\delta_e - \beta$) would be expected to be inadequate except for large ratios of base diameter to maximum diameter h/D. (As $\frac{h}{D} \rightarrow 1$ closely the use of $(\delta_e - \beta)$ as an approach would, as concluded in reference 3, be inadequate since in the limit there would be no influence of the boattail upon the base pressure.) As h/D decreases from near 1 to 0 but $\beta$ is held constant, $P_B$ will vary according to the variation of $M_0$ with h/D, which for most boattail configurations is appreciable; the same type of pressure variation that exists along the surface of the boattail has been shown in figure 17 to exist along the boundary of the convergent wake after the base, for example, from A to B in figure 13. Consequently, the assumption is made that $\beta$ is modified by some factor K and that the quantity $K\beta$ is to be subtracted from $\delta_e$. The factor K, therefore, represents essentially a conversion of $\beta$ from a three-dimensional to a two-dimensional boattail in order that it may be used with $\delta_e$, a two-dimensional quantity. An additional assumption is made that the variation of K with h/D is linear. The limits for K are established as follows: when $\frac{h}{D} = 1$, $K = 1$ since the expansion exactly at the beginning of the boattail is two dimensional; when $\frac{h}{D} = 0$, $K = 0.85$ since the empirical conversion factor of $\theta$ to $\delta_e$ was 0.85 (the latter limit may be more readily visualized by considering $\beta > \theta$). There are obviously other effects of varying h/D which will influence $P_B$, such as those discussed in the section on two-dimensional bases, which make the above limits of K a rough approximation only, particularly the limit at $\frac{h}{D} = 0$. For the

particular case of $\frac{h}{D} \to 0$ and $\beta \leq \theta$, the base would always lie near the base of the trailing shock. In addition the diametrical and axial pressure variation in the so-called dead-air region behind the base is greater for a three-dimensional than for a two-dimensional base. An indication of this conclusion may be seen in figure 22 where the distribution across a two-dimensional base and a cylindrical base of a finned parabolic body of revolution (body of ref. 18 for which fin effects were negligible) are compared. These results are from tests in the Langley 9-inch supersonic tunnel. The distribution across the two-dimensional base is seen to be almost constant, while the cylindrical base experiences appreciable variations near the edges. The variation across the cylindrical base would seem to confirm the results of force tests which have shown that pressures measured nearer the center of bases on bodies of revolution are more reliable for base drag estimations. Although no axial results are available for a two-dimensional base, the large axial pressure variations of the type shown to exist behind a three-dimensional base (fig. 17) obviously do not exist in a two-dimensional wake, otherwise there would be negligible difference in the base pressure for axially symmetric and two-dimensional flow.

In figures 23, 24, and 25 the results of several experimental measurements of the effects of conical boattailing are presented, and in figure 26 some accumulated results of measurements on the NACA RM-10 missile are presented and compared with the results obtained by the present method. For computing $P_B$ when $\beta > \theta$, the procedure employed in the two-dimensional analysis was used with $K\beta$ and $\delta_e$. In figure 23, comparison of the various methods and the experimental results for negative boattailing (simple cones) shows that all methods are fair predictions of variation and magnitude. For negative boattailing, the present method reverts to finding $P_B$ for a cone-cylinder body where the cylinder length becomes zero. For positive boattailing all methods are fair predictions of trend and magnitude through $\beta \approx 10^\circ$, though the present method indicates a variation that is slightly more in agreement with experiment. For $\beta > 10^\circ$ the present method tends to indicate the leveling off and the decrease in $P_B$ that must occur; the experimental values have also begun to level off.

In figure 24, the present method is compared with the experimental results and the method of Cortright and Schroeder. The present method was based upon the three methods employed for calculating the Mach number ahead of the base given in reference 3. The comparison shows that the prediction is very much dependent upon the method for calculating $M_o$. Both the method of Cortright and Schroeder and the present method give fair predictions of the effect of $\beta$ and the effect of $h/D$. The effect of increasing $h/D$ is seen to increase with increasing $\beta$. The present method appears to give a slightly better prediction of the

variation of $P_B$ with $\beta$ for $\frac{h}{D} = 0.704$, but this may be fortuitous, in part, since it was stated in reference 3 that at $\beta = 5.63^\circ$ the boundary layer was inadvertently thickened.

Figure 25(a) presents examples of the calculated surface pressure for various boattail angles at $M_\infty = 3.24$, and in figure 25(b) the experimental results of reference 13 are compared with the present method. Again the dependence of the method upon the theory employed to calculate $M_O$ is evident. The prediction based upon the method of characteristics is in close agreement with the experimental results.

In figure 26 fair agreement is shown in magnitude and variation between the results of the present method, for which the value of $M_O$ was calculated by the theories of Lighthill (ref. 38) and of Jones and Margolis (ref. 39), and the compilation of experimental data for the NACA RM-10 missile (parabolic body) from references 17, 31, 40, and 41. On the basis of this comparison, the present method would seem satisfactory for estimating base pressure on bodies whose boattails are not necessarily conical.

Angle-of-attack effects.- In general, the initial effect of angle of attack for bodies of revolution is to cause a decrease in base pressure until separation on the lee side of the afterbody becomes appreciable (usually near $\alpha = 15^\circ$). Further increase in $\alpha$ appears to cause a slight increase in base pressure until the angle of stall is reached (of the order of $\alpha = 35^\circ$). Indications are that at stall the base pressure experiences a decrease and, with increase in $\alpha$ beyond that for stall, remains fairly constant until $\alpha \longrightarrow 90^\circ$; near $\alpha = 90^\circ$ the base pressure must obviously increase. Both body shape and Mach number appear to have significant effects upon the variation of $P_B$ with $\alpha$. (See refs. 10 and 42, for example.) All the data examined for $\alpha > 6^\circ$ were subject to sting-interference effects; however, a preliminary investigation conducted in the Langley 9-inch supersonic tunnel indicated that sting supports designed according to existing standards so as to have small effect at $\alpha = 0^\circ$ (see refs. 2, 18, 19, and 27) may be expected to have equally small effect at angles of attack up to about $60^\circ$.

In order to assess the possibilities of the use of the present method to estimate angle-of-attack effects, the NACA RM-10 body (no fins) was selected since considerable experimental results exist for this configuration. (See refs. 40 and 41, for example.) As a point of possible interest, all the available experimental results for the RM-10 body tend to indicate that the rate of decrease in $P_B$ with $\alpha$ becomes less with increasing $M_\infty$, even for the lower values of $M_\infty$. The experimental results for the RM-10 body at $M_\infty = 1.49$ are shown in figure 27(a) and are compared with the various estimates. As a crude first-order estimate, the integrated average value of $M_O$ was

calculated using the method of Jones and Margolis (ref. 39) to determine the value of $P$ just ahead of the base at $\alpha = 0^\circ$ and the method of Allen (ref. 43), given here as

$$P_\alpha = P_{\alpha=0} + \left[4\eta\ \alpha \cos\theta + \alpha^2(1 - 4\sin^2\theta)\right] \qquad (2)$$

to determine the radial pressure distribution at the base. At each value of $\alpha$, the integrated average value of $M_o$ thus determined was used to calculate $P_B$. As shown in figure 27(a), the results indicate a decrease in $P_B$ with $\alpha$, but the rate of decrease is considerably less than experiment. This crude estimate does not take into account the possibility that a portion of the lee surface ahead of the base may have exceeded $\delta_e$, a condition that has obviously occurred at the higher angles of attack. A second and more refined estimate was made with this condition accounted for by the same method employed to estimate boattail effects; that is, at each value of $\theta$ the value of $P_B$ was determined by accounting for the boattail angle and the effective angle of attack. It was assumed that the pressure on the body surface ahead of the base was constant beyond the value of $\theta$ for separation at each $\alpha$. (See fig. 27(b).) The integrated average value of $P_B$ was calculated in this manner for each $\alpha$. The variation of $P_B$ with $\alpha$ from this second estimate is in fair agreement with the experimental results. Also shown for comparison is the variation of $P_B$ with $\alpha$ estimated by assuming that $P_B$ changes according to the change in $P$ at $\theta = 90^\circ$ as given by equation (2). The general agreement between this form of estimation and experiment was first noted in reference 40 and was concluded to be somewhat fortuitous; the same conclusion is reached here for angles of attack beyond that for separation on the lee side of the body, but for angles of attack less than that for separation this estimate should give a fair approximation since the variation in $P_B$ on the lee side of the body tends to be offset by the variation on the windward side.

In equation (2) the term in the bracket, which represents $\alpha$ effects, is independent of Mach number, but it is clear that this expression cannot be used at Mach numbers much greater than 2 since it gives a variation which would yield values of $P_B$ less than the absolute limit (vacuum). At very high Mach numbers ($M_\infty \approx 7$) Ferri's cone theory extended to the body surface would seem to be applicable. (See ref. 44.) A method applicable to the intermediate range has not been found.

## Bodies With Fins

Problem in general.- The addition of fins to a body of revolution may or may not have an appreciable effect on the base pressure. The primary variables that may influence the base pressure through the presence of the fins are: free-stream Mach number, number of fins,

fin section, fin location, fin thickness ratio, body diameter, fin sweepback, and fin span. Body shape and boattailing will, of course, interact with the above variables to affect the base pressure. There have been numerous base-pressure investigations of bodies with fins but relatively few to investigate the fin effects. Examples of the latter may be seen in references 15, 18, 20, 22, and 30.

Configuration for principal analysis.- The configuration which seems to predominate in most experimental investigations is that of references 15, 20, and 30. Additional unpublished data for a similar configuration have recently been obtained in the Langley 9-inch supersonic tunnel and are presented herein. The basic configuration consists of a cylindrical body equipped with an ogival nose and four equally spaced 10-percent-thick fins having symmetrical circular-arc sections and rectangular plan forms. The ratio of fin span to body diameter is 3.5, the ratio of fin thickness to body diameter is 0.15, and the trailing edges of the fins are coincident with the base. The original full-scale models were tested in free flight and were reported on in references 15 and 20. In reference 30, a foreshortened model was tested in a wind tunnel to determine the effects of fin location, fin thickness, and number of fins. For the tests in the Langley 9-inch supersonic wind tunnel the nose of the body was conical, but was far enough ahead of the fins to have negligible effect on the base pressure from nose shape. In addition, the body extended one fin-chord length behind the fin trailing edge. Measurements were made of the pressure field on the body surface created by the presence of the fins. Less extensive direct measurements were made of the effects of fin location on base pressure.

Effects of fin location and Mach number.- Figure 28 presents the results of the pressure measurements on the body surface at Mach numbers of 1.93 and 2.41 for Reynolds numbers of approximately $3 \times 10^6$ and $12 \times 10^6$. For the lower Reynolds number laminar flow existed ahead of the fin-body juncture which caused turbulent flow in the manner described in reference 18. At the higher Reynolds number natural transition occurred considerably ahead of the fin-body juncture. The results at $M_\infty = 1.93$ show that Reynolds number had little effect on the body pressures, whereas at $M_\infty = 2.41$ the higher Reynolds number gave consistently higher body pressures.

In order to determine whether an average Mach number ahead of the base could be used to predict the base pressure, the surface pressure coefficients of figure 28 for the higher Reynolds number were employed to obtain the integrated average Mach number ahead of the base shown in figure 29. The values of $x/c$ define the location with respect to the base of the trailing edge of the fin in terms of fin chord and agree with the convention used in reference 30. Utilizing the present

method for predicting base pressures, the values of $P_B$ shown in figure 30 were computed. In reference 30 experimental values of $P_B$ were obtained at Mach numbers 1.5 and 2.0 with varying x/c. These values may be subject to some effects from nose shape, particularly for the large positive values of x/c, since the relation of the body-alone pressure distribution (for M = 2.00) to the geometry of the configuration is as shown in figure 31. However, a preliminary investigation of the effect of body length in reference 30 seems to indicate that these effects would be small. Also, as shown in figure 31, at negative x/c the base of the fins protruded into the dead-air region behind the base and may have some effect on the experimental values of $P_B$. From the comparisons to follow, however, these effects would also seem to be small.

Figure 32 presents several comparisons of predicted and experimental values of $P_B$ for the finned body as x/c is varied. The experimental results obtained in reference 30 at $M_\infty = 1.50$ and 2.00 are shown as the dot-dash curves extending over a range of $\frac{x}{c} = \pm 1$. A comparison of the curve at $M_\infty = 2.00$ with the calculated curve of figure 30 for $M_\infty = 1.93$ indicated an almost exact prediction of the variation in base pressure if the calculated curve were shifted downstream by $\frac{x}{c} \approx 0.5$. The calculated curve shifted by this amount is shown in figure 32. Although the agreement in variation with x/c is good, the predicted values of base pressure for $M_\infty = 1.93$ would appear to be slightly high when compared with the experimental values for $M_\infty = 2.00$. At $M_\infty = 2.41$ the experimental measurements of $P_B$ were confined to positive x/c. Though the justification is not as strong as for the previous comparison, a shift of the predicted curve downstream by $\frac{x}{c} \approx 0.6$ gives a general agreement with the experimental variation in the overlapping range of positive x/c. As before, the predicted values of base pressure are somewhat high.

In spite of the shortcomings of the above comparisons, several indications of various fin effects are shown. The most important finding here seems to be that whereas for unfinned bodies, including those of small fineness ratio, the base pressure may be reasonably predicted when the Mach number and pressure ahead of the base are known, for the finned body of this investigation the integrated average Mach number ahead of the base predicts the proper variation of base pressure with fin location only when the predicted variation is shifted rearward. Consequently, the conclusion may be drawn that the effects of the pressure fields created by the fins have appreciable effect on the wake boundaries behind the base and must be taken into account. In addition, the magnitude of the prediction of $P_B$ from the integrated average value of $M_O$ is of the right order when the distance through which the predicted curve must be shifted is known. The effect of

increasing Mach number is to lessen the fin effects at a given value of $x/c$ and to extend further downstream the region of influence from the fins; both of these effects would be expected since increasing Mach number reduces thickness effects and causes the regions of disturbance from a point to be swept farther back. From the results of figure 32, the effect of increasing body diameter while all other parameters are held constant may be reasoned to result generally in a reduction of the fin effects upon the base pressure.

Effects of thickness ratio and sweepback of fins.- Figure 33 presents the variation in base pressure resulting from a variation in thickness ratio of the fins for this configuration. All data are for a fin position of $\frac{x}{c} = 0$. The effect of increasing $t/c$ in decreasing the base pressure is seen to be significant. Also indicated is the reduction of this effect from increasing Mach number. In view of these effects, giving sweepback to the fins would, in most instances, decrease the fin effects upon base pressure since, effectively, the thickness ratio of the fin parallel to the body surface is reduced. The results of reference 18 when compared with the results of the present investigation for similar fin locations, and with proper consideration of thickness as shown in figure 33, demonstrate clearly the reduced fin effects resulting from sweeping the fins back $45^\circ$. Figure 34 gives an example of the relatively small effects of the fins of the NACA RM-10 missile, which are 10 percent thick and sweptback $60^\circ$.

Some estimations of fin effects.- In an effort to determine whether the pressure field due to the fins for the configuration under discussion could be approximated reasonably by simple shock-expansion theory, and thereby make some crude approximations of the fin effects on base pressure for $\frac{x}{c} = 0$ over the Mach number range of the results of references 15 and 20, the integrated average Mach number ahead of the base was determined by graphically constructing the expansion field about a fin at $M_\infty = 2.00$ for a range of $\frac{x}{c} = \pm 1$. The resulting estimation of $P_B$ (shifted downstream by $\frac{x}{c} = 0.5$ as before) is entered on figure 32 and compared with the experimental results. From $\frac{x}{c} = 0$ to $\frac{x}{c} = -1.0$ the estimation is fair. The high pressure peak beyond $\frac{x}{c} = -1.0$ appears invalid, though it is a crude prediction of trend; the values for $\frac{x}{c} > 0$ are unsatisfactory. On the basis of the fair prediction from $\frac{x}{c} = 0$ to $\frac{x}{c} = -1.0$, this method has been used in the predictions to be discussed in the following paragraph.

Figure 35 presents a comparison of the free-flight results for the configuration under discussion (from ref. 15) and two predictions

utilizing the present method based upon the integrated average Mach number at certain $x/c$ stations. Also included for comparison are the wind-tunnel results, with and without fins, from the tests in the Langley 9-inch supersonic tunnel and those reported in reference 30, and the body-alone curve from figure 18. Referring to figure 32, the amount of displacement in the predicted curves necessary to bring them in line with the experimental variations is seen to be equivalent to the negative value of $x/c$ at which the minimum base pressure occurs. One of the predicted curves of figure 35 (estimate A) is based upon this displacement. The location of the minimum base pressure at negative $x/c$ plotted against Mach number gives essentially a linear variation with $M_\infty$, and this assumed linear variation has been used to select the value of $x/c$ for which the integrated average $M_O$ was calculated for estimating $P_B$. For example, at $M = 2.00$ the value of $x/c$ to be used is about 0.51, and at $M = 1.50$ it is approximately 0.4. (The stations for calculation must be positive since the curve is always shifted to the right.) Essentially, therefore, the value of $M_O$ thus obtained corresponds to a station behind the base and along a fictitious extension of the body surface, and in this regard supports the method of Chapman (ref. 2).

The other predicted curve in figure 35 (estimate B) was obtained by a somewhat different method in that the station behind the base, but along a fictitious extension of the body, was chosen differently. In reference 2, measurements were made of the wake thickness behind cone-cylinder bodies of fineness ratio 5. The faired curve from these measurements is shown in figure 36(a) in terms of base diameter. The wake thickness $t_W$ was measured just behind the trailing shock since in this region $t_W$ is almost constant and is well defined. These values of $t_W$ have been used with the values of $\theta$ from figure 14 to calculate an approximation of the location of the base of the trailing shock in terms of body diameters from the base. The results are shown in figure 36(b). (It is interesting to note that although $t_W$ and $\theta$ may vary appreciably with $M_\infty$, the approximate location of the base of the trailing shock experiences little change.) The assumption was made that disturbances from the fins would have no effect on $P_B$ beyond a value of $x/c$ corresponding to the location of the base of the trailing shock thus determined. The station behind the base along the fictitious body extension selected for calculating $M_O$ was halfway between the base of the body and the base of the trailing shock, or if the last expansion from the fin did not reach $\frac{x}{c} = \frac{N}{h}$ (low $M_\infty$), the station was halfway between the base and the intersection of the last expansion from the fin with the extended body (meridian $45^\circ$ from meridian of fin).

As shown in figure 35 the former estimate (labeled estimate A) is more in agreement with experiment at the higher Mach numbers while the latter estimate (estimate B) tends to be more satisfactory at the

lower Mach numbers. Even though these approximations are based on simple approaches, both give a fair estimation of the fin effects. No calculations were made below $M_\infty = 1.5$ since the leading-edge shock on the fins is near detachment. Shock detachment and the interaction of the shocks from opposite fins may explain why the experimental results tend to level off at the lower Mach numbers. All of the wind-tunnel base pressures for the finned body are lower than the free-flight results. The body-alone results are in fair agreement with the curve from figure 18 with the possible exception of the point at $M = 1.5$. Also indicated is the decrease in fin effects as Mach number increases.

General remarks.- It is possible to visualize that for certain conditions the fins would have small or negligible effect on base pressure until moderate or high Mach numbers are reached. For example, a fin could be of such a design and so located with respect to the base that at low Mach numbers only small effects would be experienced by $P_B$ due to the localization of the region of primary influence. At higher Mach numbers the downstream extension of the region of primary influence could cause a decrease in base pressure. Such a variation has been measured in the vicinity of $M_\infty = 2.6$ on finned free-flight models and reported in reference 24.

There is a need for much additional experimental information on the effects of the variables associated with fins upon the base pressure. Even though the simplified approach presented herein gives fair approximations of the pressures created by the fins, a more rigorous method would aid considerably in attempts to analyze the fin effects. The method of Moskowitz and Maslen (ref. 45) may, when modified to apply to cruciform fins, give a sufficiently accurate prediction of the pressures on the body surface to aid in such an analysis; in view of the rather lengthy calculations involved and the fact that the agreement between prediction and experiment shown in reference 45 was, in some instances, only fair, no attempt was made to extend the method to this investigation.

## CONCLUDING REMARKS

A summary analysis has been made of available experimental data to show the effects of most of the variables that are more predominent in influencing base pressure at supersonic speeds on two-dimensional bases and the bases of bodies of revolution, with and without fins, having turbulent boundary layers. In this analysis an attempt has also been made to show the present status of available experimental information on base pressure and the methods for its prediction.

A simple semiempirical method is presented for estimating base pressure that essentially extends the method of Cortright and Schroeder (NACA RM E51F26), and which for two-dimensional bases, stems from an analogy established between the base-pressure phenomena and the pressure rise required to separate the boundary layer. An analysis is made for axially symmetric flow which indicates that the base pressure for bodies of revolution is subject to the same analogy. Based upon the methods presented, estimations are made of such effects as Mach number, angle of attack, boattailing, fineness ratio, and fin effects. These estimations are fair predictions of experimental results.

There appear to be few systematic investigations of the effects of fins upon base pressure. The complexity of this problem and the many variables involved would seem to warrant equal if not more attention in experimental and theoretical investigations than that being devoted to bodies without fins.

Langley Aeronautical Laboratory,
National Advisory Committee for Aeronautics,
Langley Field, Va.

## REFERENCES


1. Crocco, Luigi, and Lees, Lester: A Mixing Theory for the Interaction Between Dissipative Flows and Nearly-Isentropic Streams. Rep. No. 187, Princeton Univ., Aero. Eng. Lab., Jan. 15, 1952.

2. Chapman, Dean R.: An Analysis of Base Pressure at Supersonic Velocities and Comparison With Experiment. NACA Rep. 1051, 1951. (Supersedes NACA TN 2137.)

3. Cortright, Edgar M., Jr., and Schroeder, Albert H.: Investigation at Mach Number 1.91 of Side and Base Pressure Distributions Over Conical Boattails Without and With Jet Flow Issuing From Base. NACA RM E51F26, 1951.

4. Gabeaud, A.: Base Pressures at Supersonic Velocities. Jour. Aero. Sci. (Readers' Forum), vol. 17, no. 8, Aug. 1950, pp. 525-526.

5. Cope, W. F.: The Effect of Reynolds Number on the Base Pressure of Projectiles. Eng. Div. 63/44, NPL, British A.R.C., Jan. 1945.

6. Kurzweg, H. H.: Interrelationship Between Boundary Layer and Base Pressure. Jour. Aero. Sci., vol. 18, no. 11, Nov. 1951, pp. 743-748.

7. Gabeaud, [A.]: Base Pressures at Supersonic Velocities. Jour. Aero. Sci. (Readers' Forum), vol. 16, no. 10, Oct. 1949, p. 638.

8. Lorenz, H.: Der Geschosswiderstand. Physikalische Zeitschrift, vol. 18, 1917, p. 209; vol. 29, 1928, p. 437.

9. Von Kármán, Theodor, and Moore, Norton B.: Resistance of Slender Bodies Moving With Supersonic Velocities With Special Reference to Projectiles. Trans. A.S.M.E., vol. 54, no. 23, Dec. 15, 1932, pp. 303-310.

10. Seiff, Alvin, Sandahl, Carl A., Chapman, Dean R., Perkins, E. W., and Gowen, F. E.: Aerodynamic Characteristics of Bodies at Supersonic Speeds. A Collection of Three Papers. NACA RM A51J25, 1951.

11. Chapman, Dean R., and Perkins, Edward W.: Experimental Investigation of the Effects of Viscosity on the Drag and Base Pressure of Bodies of Revolution at a Mach Number of 1.5. NACA Rep. 1036, 1951. (Supersedes NACA RM A7A31a.)

12. Chapman, Dean R., Wimbrow, William R., and Kester, Robert H.: Experimental Investigation of Base Pressure on Blunt-Trailing-Edge Wings at Supersonic Velocities. NACA TN 2611, 1952.

13. Kurzweg, H. H.: The Base Pressure Measurements of Heated, Cooled, and Boat-Tailed Models at Mach Numbers 1.5 to 5.0. NAVORD Rep. 1651, Proc. of the Bur. of Ord. Symposium on Aeroballistics. (Defense Res. Lab. Rep. No. 267), Univ. Texas, Nov. 16-17, 1950, pp. 119-142.

14. Boreli, F.: Druckverteilungsmessungen an Geschossmodellen. UM Nr. 6057, Aerodynamisches Institut T. H. Aachen, Mar. 6, 1945. (Available in English translation from CADO, ATI 2457 as Douglas Aircraft Co., Inc., Rep. No. F.R. 340, 1947.)

15. Faro, I. D. V.: Experimental Determination of Base Pressures at Supersonic Velocities. Bumblebee Rep. No. 106, The Johns Hopkins Univ., Appl. Phys. Lab., Nov. 1949.

16. Hoerner, Sighard F.: Base Drag and Thick Trailing Edges. Jour. Aero. Sci., vol. 17, no. 10, Oct. 1950, pp. 622-628.

17. Love, Eugene S., Coletti, Donald E., and Bromm, August F., Jr.: Investigation of the Variation With Reynolds Number of the Base, Wave, and Skin-Friction Drag of a Parabolic Body of Revolution (NACA RM-10) at Mach Numbers of 1.62, 1.93, and 2.41 in the Langley 9-Inch Supersonic Tunnel. NACA RM L52H21, 1952.

18. Love, Eugene S., and O'Donnell, Robert M.: Investigations at Supersonic Speeds of the Base Pressure on Bodies of Revolution With and Without Sweptback Stabilizing Fins. NACA RM L52J21a, 1952.

19. Perkins, Edward W.: Experimental Investigation of the Effects of Support Interference on the Drag of Bodies of Revolution at a Mach Number of 1.5. NACA TN 2292, 1951.

20. Hill, Freeman K., and Alpher, Ralph A.: Base Pressures at Supersonic Velocities. Jour. Aero. Sci., vol. 16, no. 3, Mar. 1949, pp. 153-160.

21. Charters, A. C., and Turetsky, R. A.: Determination of Base Pressure From Free-Flight Data. Rep 653, Ballistic Res. Lab., Aberdeen Proving Ground, 1948.

22. Hart, Roger G.: Effects of Stabilizing Fins and a Rear-Support Sting on the Base Pressures of a Body of Revolution in Free Flight at Mach Numbers from 0.7 to 1.3. NACA RM L52E06, 1952.

23. Peck, Robert F.: Flight Measurements of Base Pressure on Bodies of Revolution With and Without Simulated Rocket Chambers. NACA RM L50I28a, 1950.

24. Jackson, H. Herbert, Rumsey, Charles B., and Chauvin, Leo T.: Flight Measurements of Drag and Base Pressure of a Fin-Stabilized Parabolic Body of Revolution (NACA RM-10) at Different Reynolds Numbers and at Mach Numbers From 0.9 to 3.3. NACA RM L50G24, 1950.

25. Katz, Ellis R., and Stoney, William E., Jr.: Base Pressures Measured on Several Parabolic-Arc Bodies of Revolution in Free Flight at Mach Numbers From 0.8 to 1.4 and at Large Reynolds Numbers. NACA RM L51F29, 1951.

26. Ferri, Antonio: Supersonic-Tunnel Tests of Projectiles in Germany and Italy. NACA WR L-152, 1945. (Formerly NACA ACR L5H08.)

27. Reller, John O., Jr., and Hamaker, Frank M.: An Experimental Investigation of the Base Pressure Characteristics of Nonlifting Bodies of Revolution at Mach Numbers From 2.73 to 4.98. NACA RM A52E20, 1952.

28. Hill, F. K.: Base Pressures at a Mach Number of 5.1. APL/JHU/CF-1306, Johns Hopkins Univ., Appl. Phys. Lab., July 11, 1949.

29. Goin, Kennith L.: Effects of Plan Form, Airfoil Section, and Angle of Attack on the Pressure Along the Base of Blunt-Trailing-Edge Wings at Mach Numbers of 1.41, 1.62, and 1.96. NACA RM L52D21, 1952.

30. Spahr, J. Richard, and Dickey, Robert R.: Effect of Tail Surfaces on the Base Drag of a Body of Revolution at Mach Numbers of 1.5 and 2.0. NACA TN 2360, 1951.

31. Czarnecki, K. R., and Marte, Jack E.: Skin-Friction and Boundary-Layer Transition on a Parabolic Body of Revolution (NACA RM-10) at a Mach Number of 1.6 in the Langley 4- by 4-Foot Supersonic Pressure Tunnel. NACA RM L52C24, 1952.

32. Bogdonoff, Seymour M.: A Preliminary Study of Reynolds Number Effects on Base Pressure at $M = 2.95$. Jour. Aero. Sci., vol. 19, no. 3, Mar. 1952, pp. 201-206.

33. Morrow, John D., and Katz, Ellis: Flight Investigation at Mach Numbers From 0.6 to 1.7 To Determine Drag and Base Pressures on a Blunt-Trailing-Edge Airfoil and Drag of Diamond and Circular-Arc Airfoils at Zero Lift. NACA RM L50E19a, 1950.

34. Donaldson, Coleman duP., and Lange, Roy H.: Study of the Pressure Rise Across Shock Waves Required To Separate Laminar and Turbulent Boundary Layers. NACA TN 2770, 1952.

35. Prandtl, L.: The Mechanics of Viscous Fluids. Vol. III of Aerodynamic Theory, div. G, sec. 18, W. F. Durand, ed., Julius Springer (Berlin), 1935, pp. 112-119.

36. Beastall, D., and Eggink, H.: Some Experiments on Breakaway in Supersonic Flow (Part II). TN No. Aero. 2061, British R.A.E., June 1950.

37. Chapman, Dean R.: Note on Base Pressure Measurements. Jour. Aero. Sci. (Readers' Forum), vol. 17, no. 12, Dec., 1950, pp. 812-813.

38. Lighthill, M. J.: Supersonic Flow Past Bodies of Revolutions. R. & M. No. 2003, British A.R.C., 1945.

39. Jones, Robert T., and Margolis, Kenneth: Flow Over a Slender Body of Revolution at Supersonic Velocities. NACA TN 1081, 1946.

40. Luidens, Roger W., and Simon, Paul C.: Aerodynamic Characteristics of NACA RM-10 Missile in 8- by 6-Foot Supersonic Wind Tunnel at Mach Numbers From 1.49 to 1.98. I - Presentation and Analysis of Pressure Measurements (Stabilizing Fins Removed). NACA RM E50D10, 1950.

41. Esenwein, Fred T., Obery, Leonard J., and Schueller, Carl F.: Aerodynamic Characteristics of NACA RM-10 Missile in 8- by 6-Foot Supersonic Wind Tunnel at Mach Numbers From 1.49 to 1.98. II - Presentation and Analysis of Force Measurements. NACA RM E50D28, 1950.

42. Cohen, Robert J.: Aerodynamic Characteristics of Four Bodies of Revolution Showing Some Effects of Afterbody Shape and Fineness Ratio at Free-Stream Mach Numbers From 1.50 to 1.99. NACA RM E51C06, 1951.

43. Allen, H. Julian: Pressure Distribution and Some Effects of Viscosity on Slender Inclined Bodies of Revolution. NACA TN 2044, 1950.

44. Cooper, Ralph D., and Robinson, Raymond A.: An Investigation of the Aerodynamic Characteristics of a Series of Cone-Cylinder Configurations at a Mach Number of 6.86. NACA RM L51J09, 1951.

45. Moskowitz, Barry, and Maslen, Stephen H.: Experimental Pressure Distributions Over Two Wing-Body Combinations at Mach Number 1.9. NACA RM E50J09, 1951.

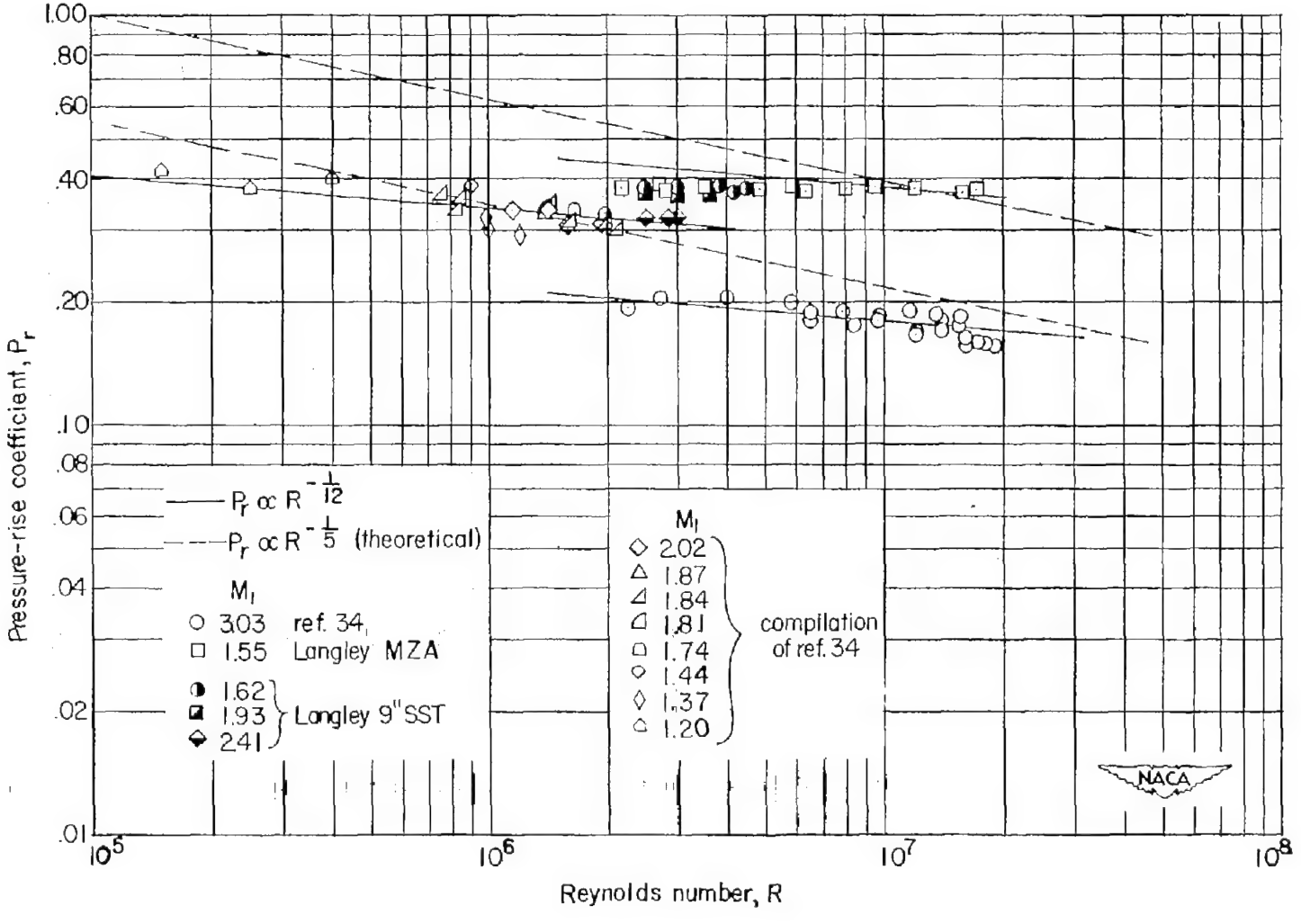


Figure 1.- Effect of Reynolds number upon the pressure rise through a shock required to separate the turbulent boundary layer on a flat plate.

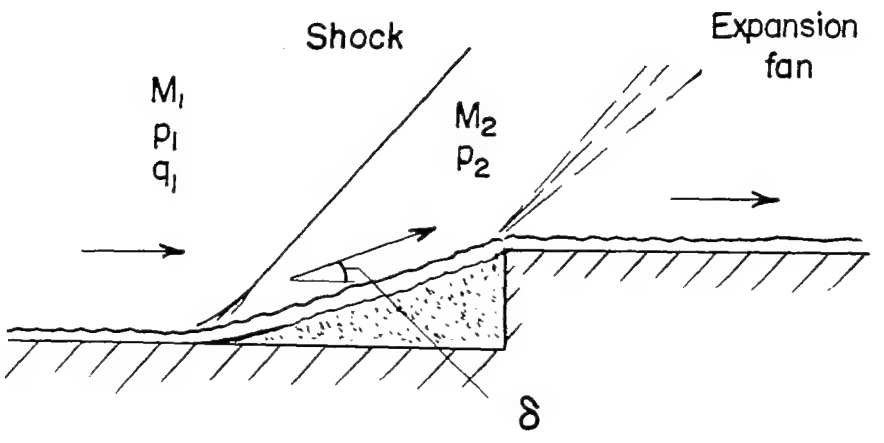


$$\text{Pressure-rise coefficient, } P_r = \frac{p_2 - p_1}{q_1}$$

(a) Sketch of separation phenomena on a flat plate caused by a forward-facing step.

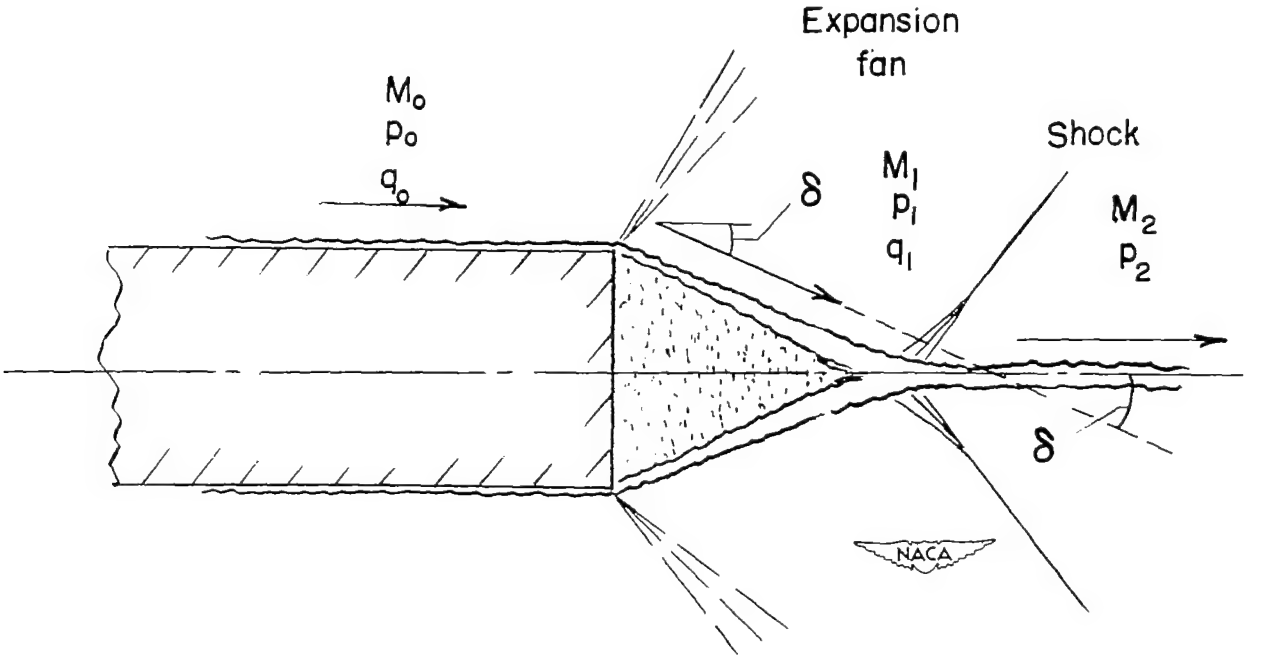


(b) Sketch of phenomena behind a two-dimensional base.

Figure 2.- Analogy between flow phenomena for forward-facing step and two-dimensional base.

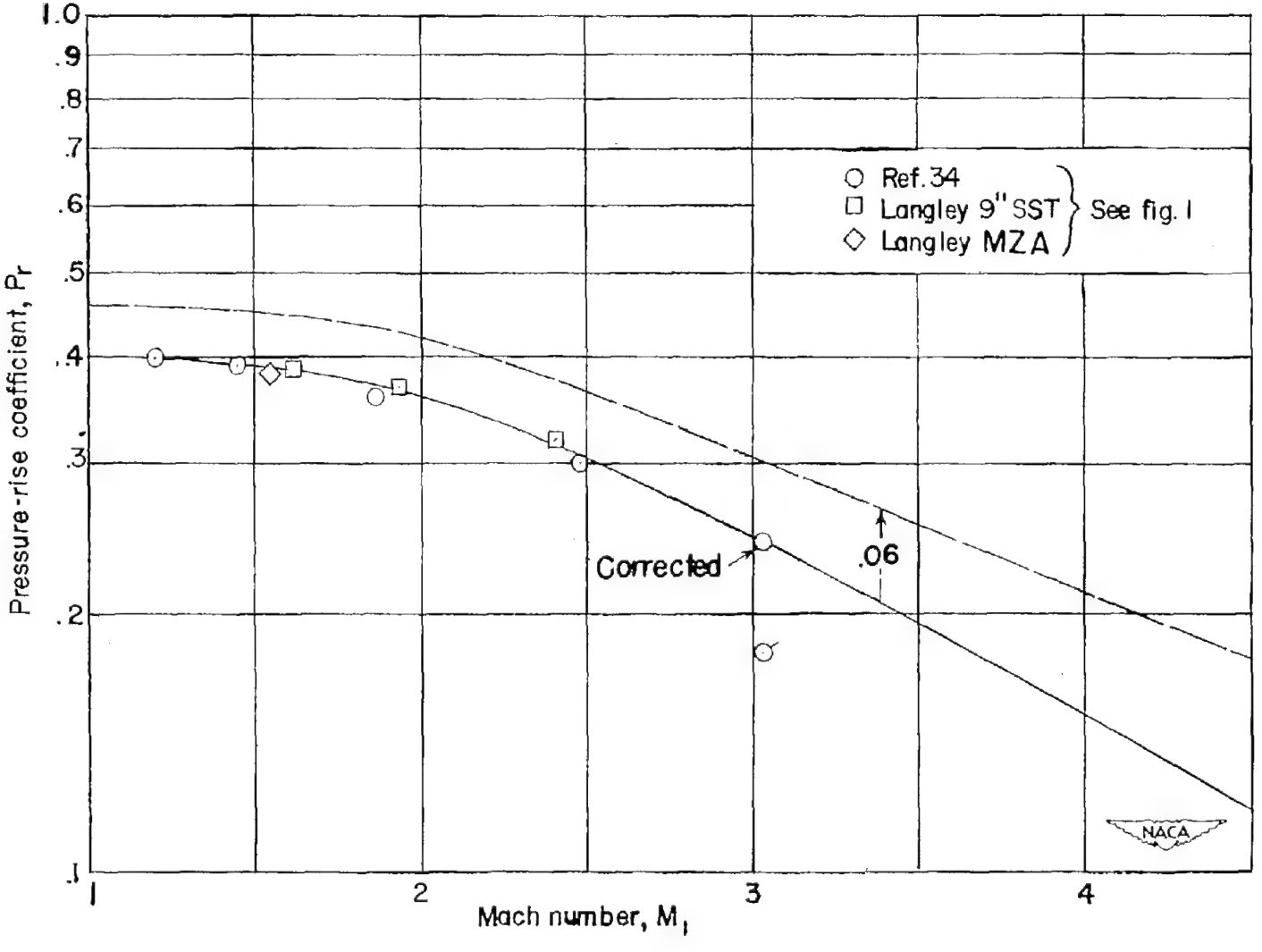


Figure 3.- Pressure rise through a shock required to separate the turbulent boundary layer on a flat plate.

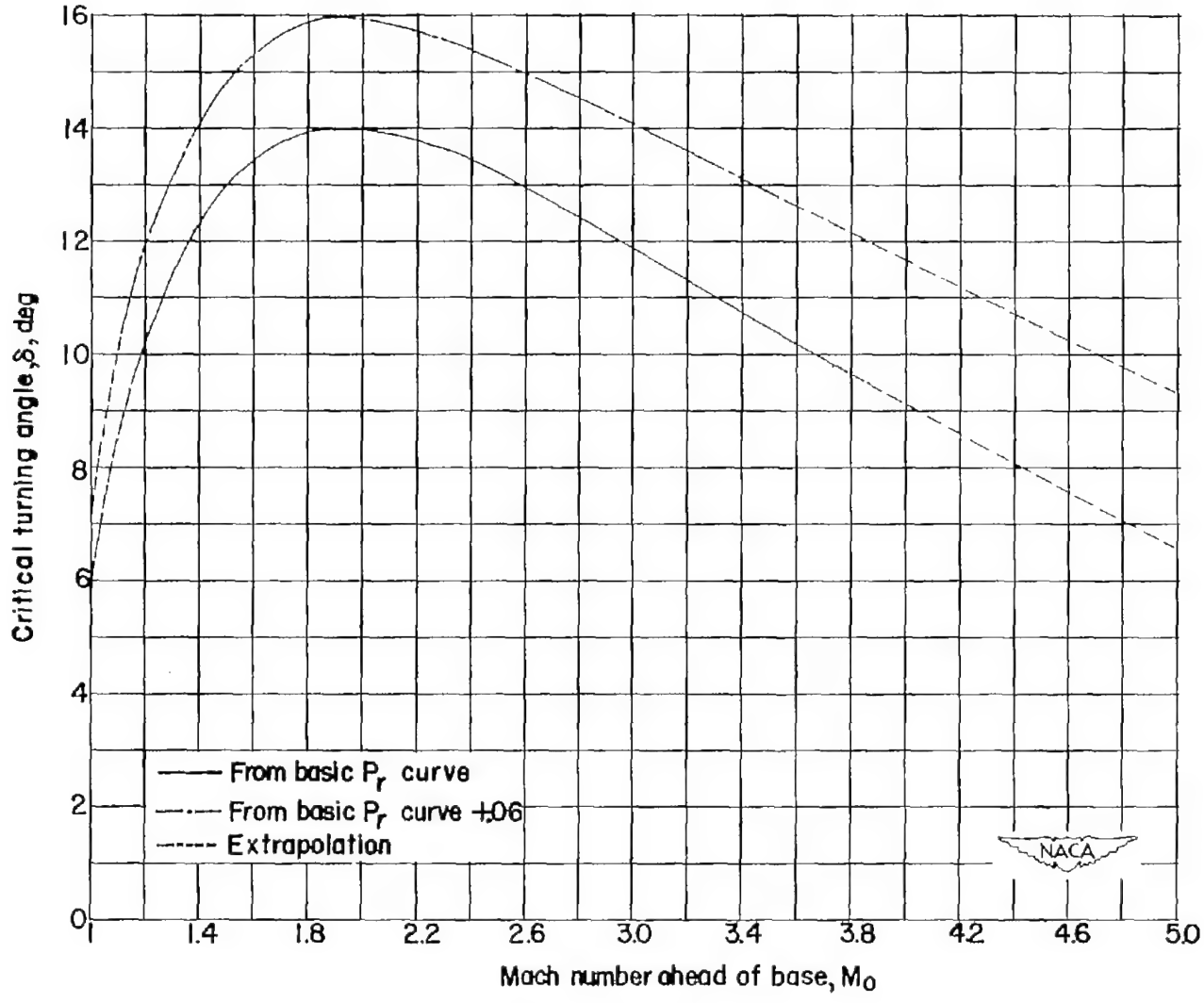


Figure 4.- Critical turning angle δ corresponding to pressure rise required to separate the boundary layer.

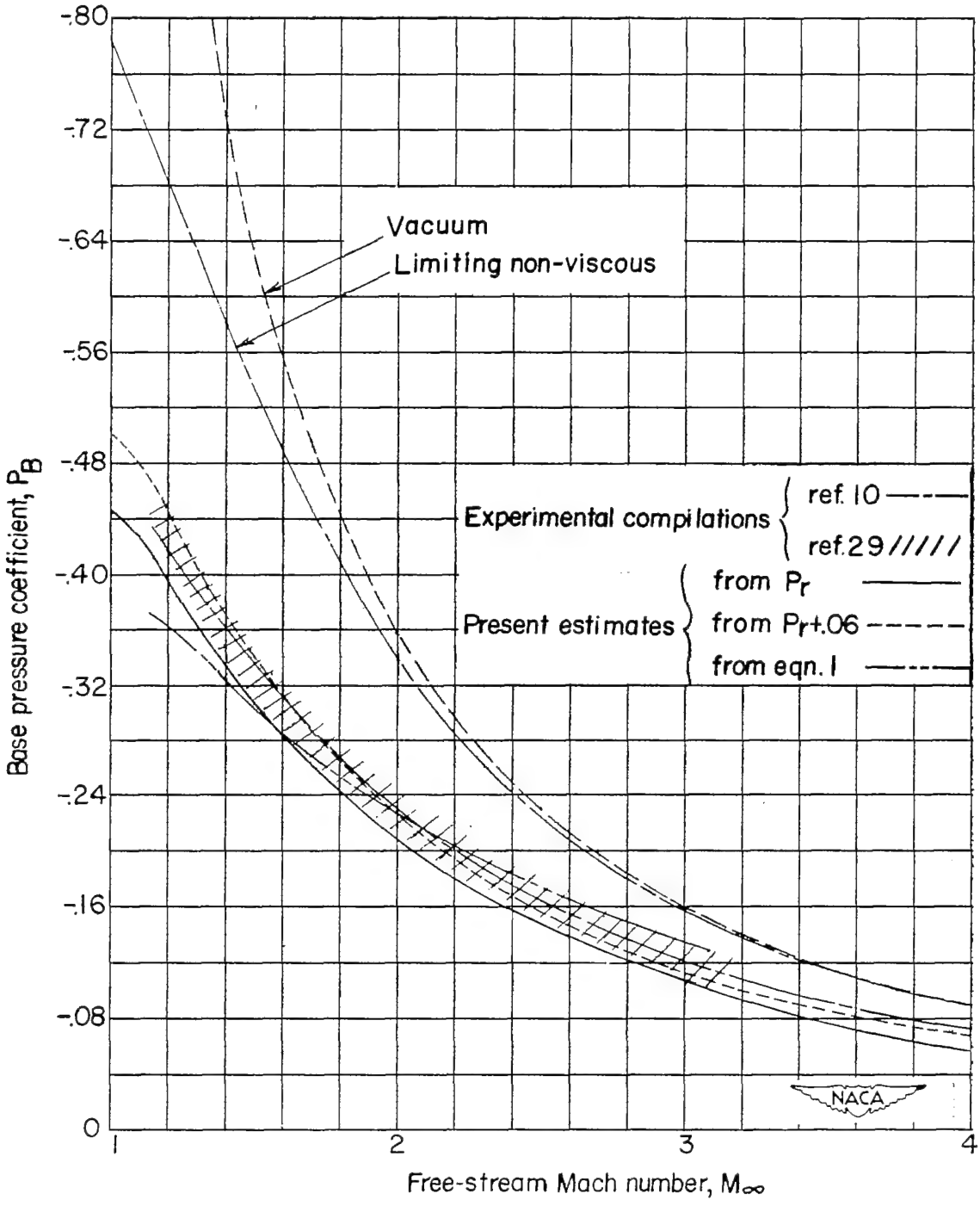


Figure 5.- Two-dimensional base pressures.

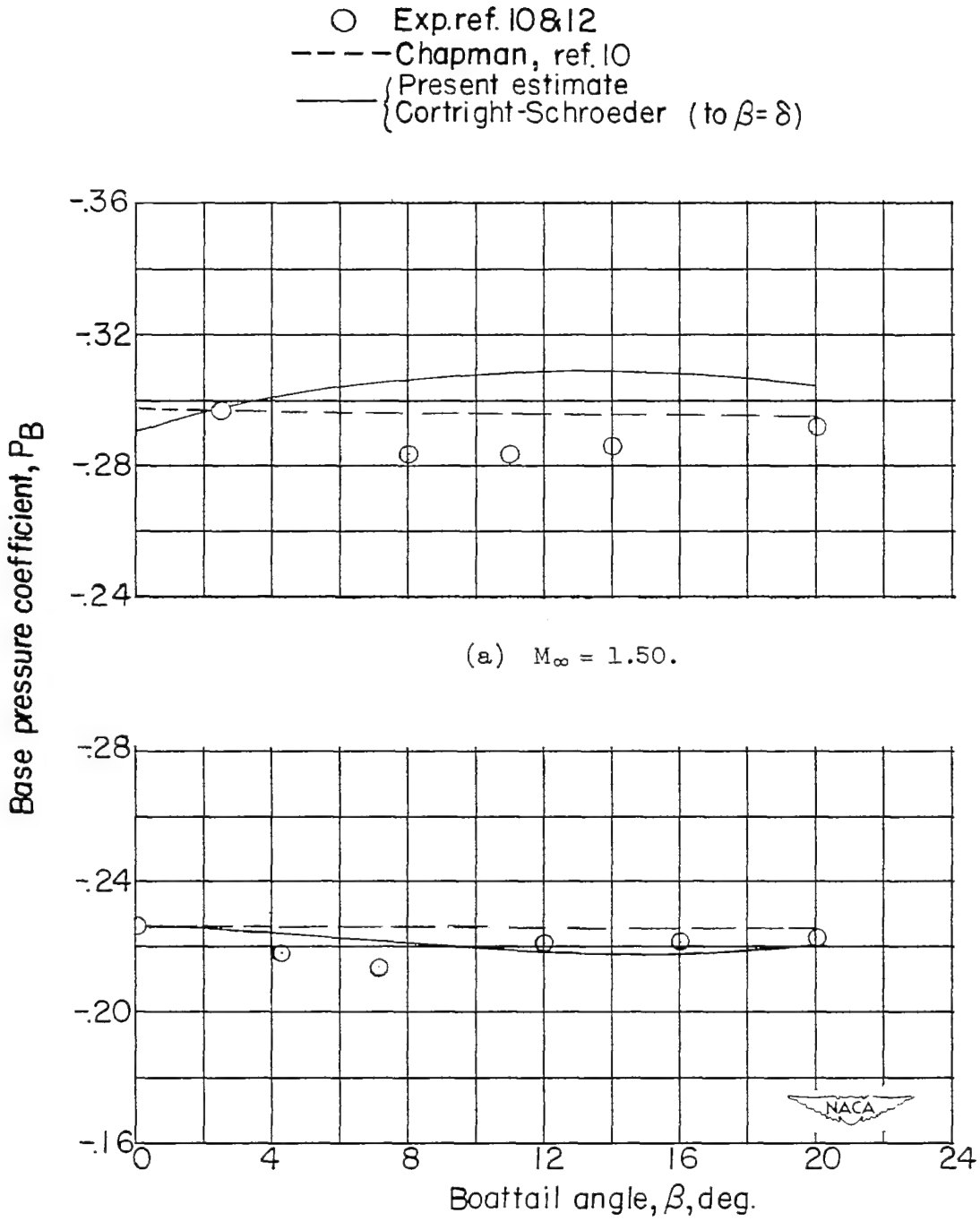


Figure 6.- Effects of boattailing on two-dimensional base pressures. $M_\infty$ = 1.50 and 2.00.

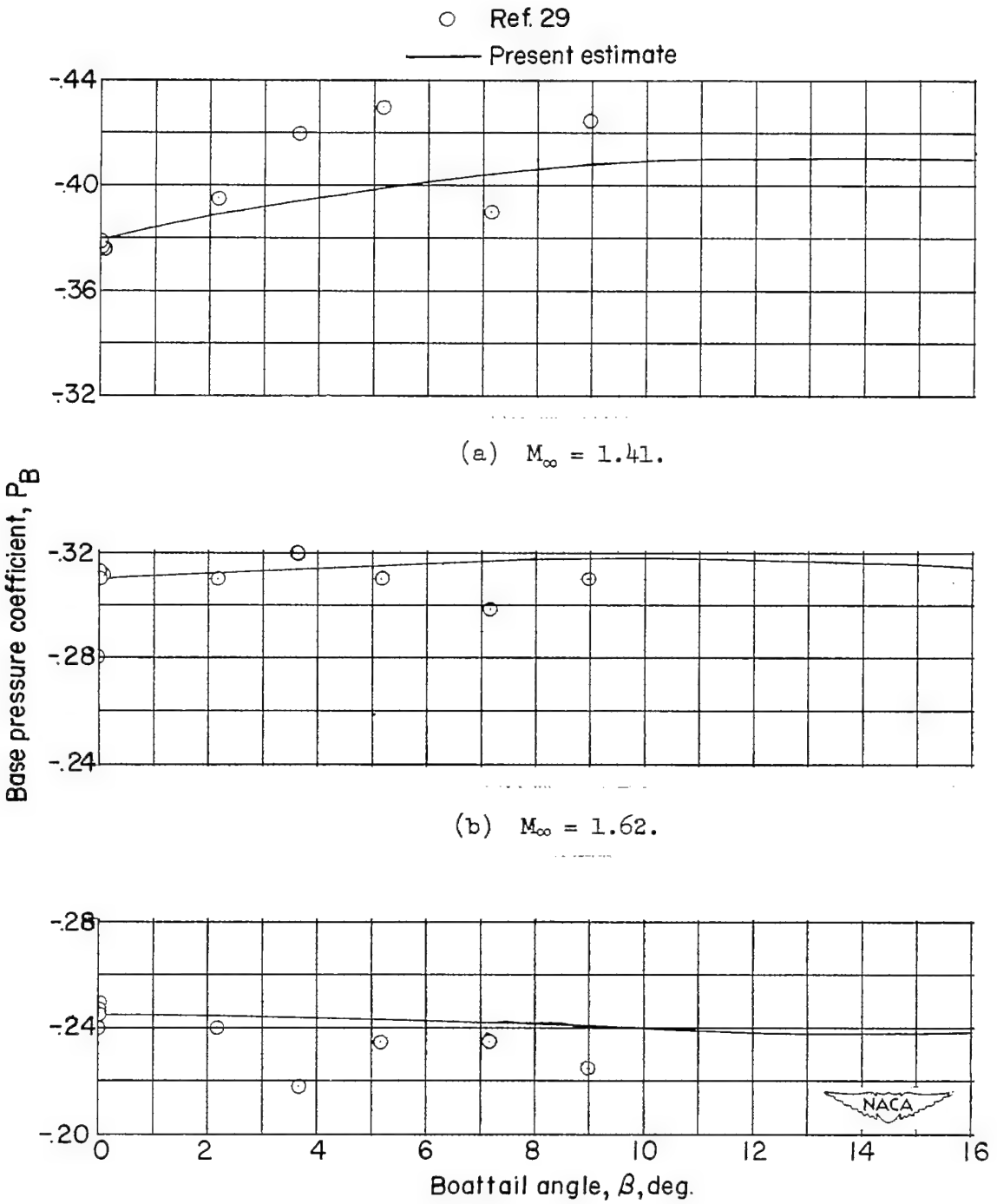


(a) $M_\infty = 1.41$.

(b) $M_\infty = 1.62$.

(c) $M_\infty = 1.96$.

Figure 7.- Effects of boattailing on two-dimensional base pressures, $M_\infty = 1.41$, 1.62, and 1.96.

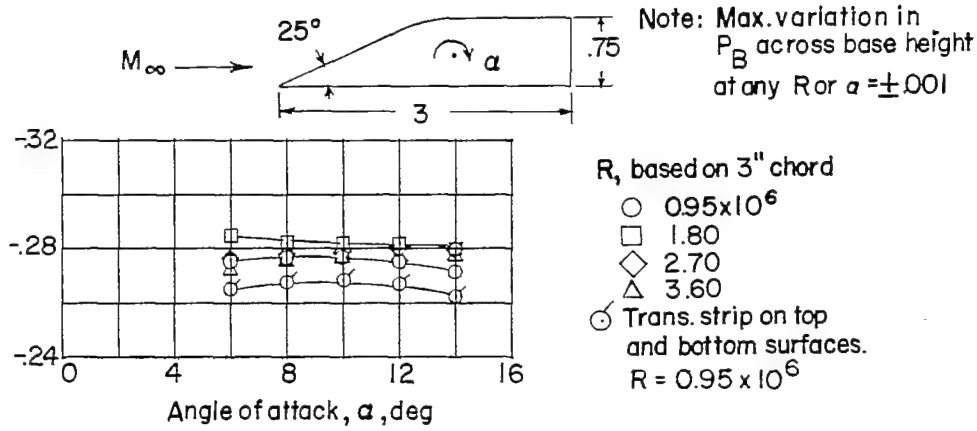


(a) $M_\infty = 1.93$.

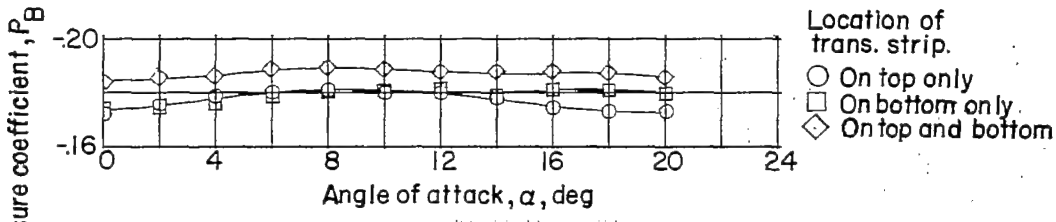


(b) $M_\infty = 2.41$, $R = 0.25 \times 10^6$.

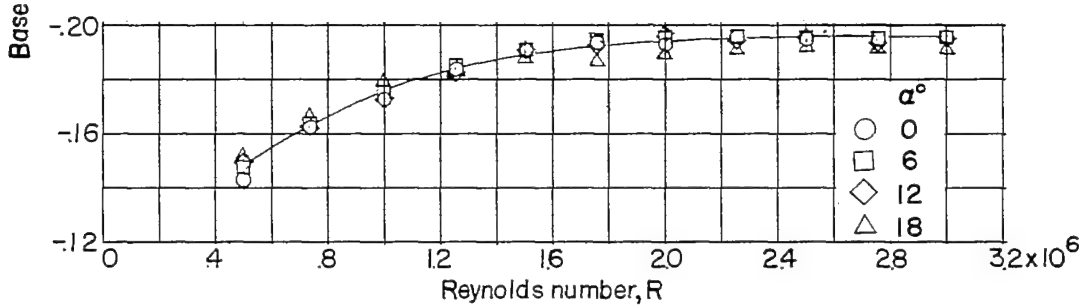


(c) $M_\infty = 2.41$.

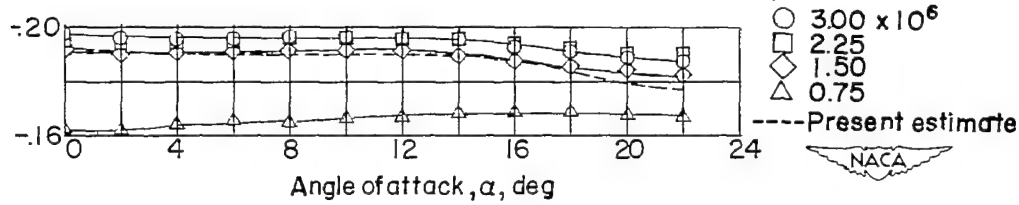


(d) $M_\infty = 2.41$.

Figure 8.- Some effects of angle of attack on two-dimensional base pressures, $M_\infty = 1.93$ and 2.41.

(a) Vertical knife-edge schlieren photographs showing vortex street in wake. ($\alpha$=10° trans. strip on top and bottom surfaces.)

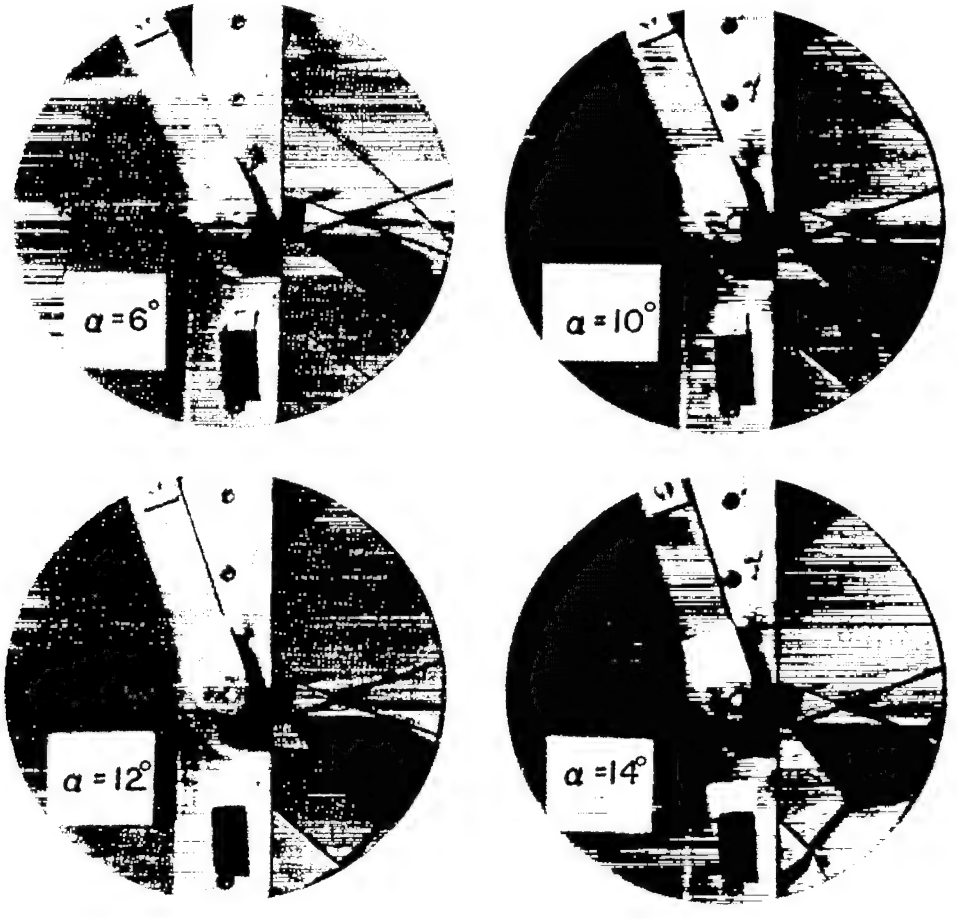


(b) Shadowgraphs showing effect of angle of attack on the base phenomena ($R = 1.80 \times 10^6$)

NACA L-77943

Figure 9.- Flow phenomena behind two-dimensional base. $M_\infty = 1.93$.

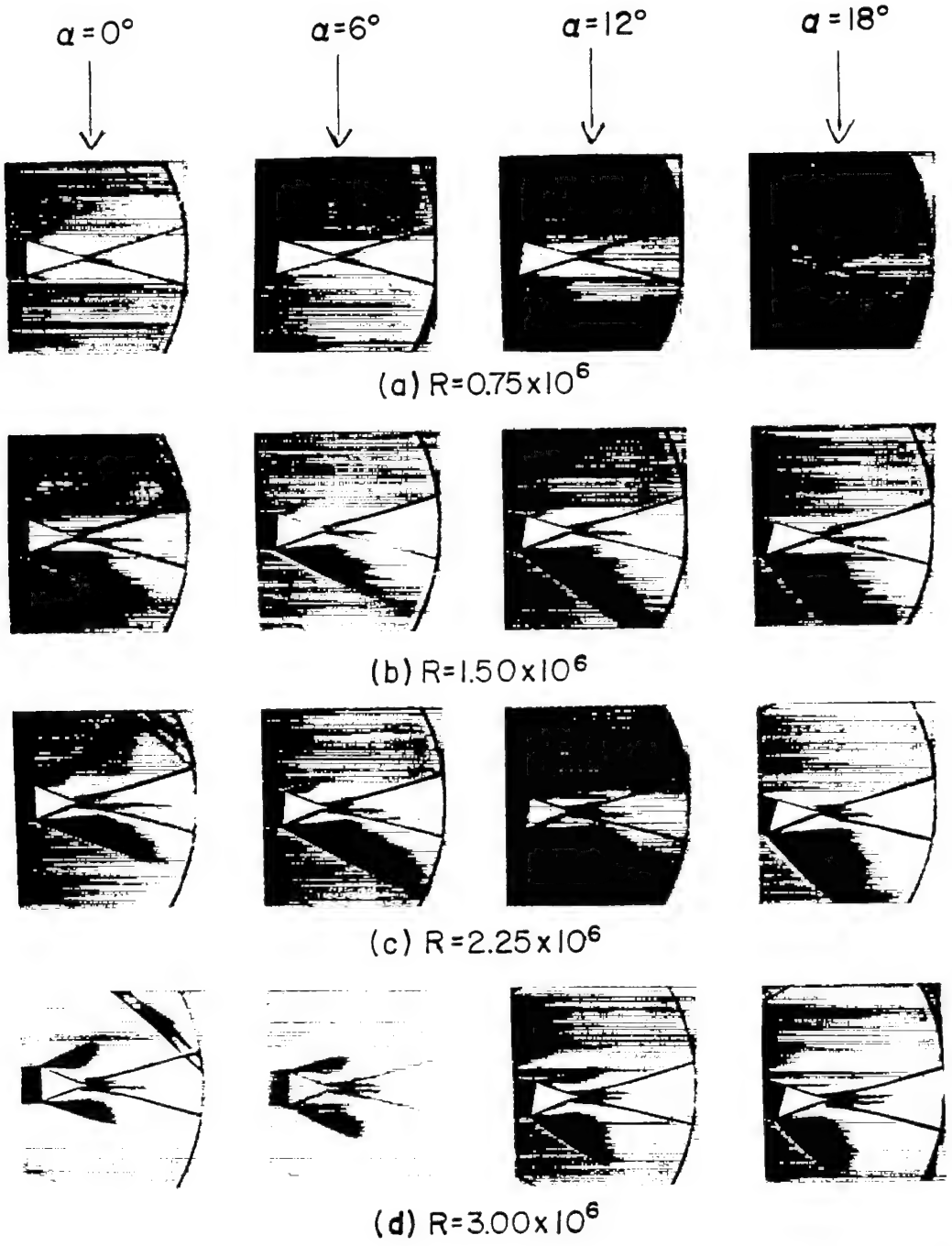


Figure 10.- Flow phenomena behind two-dimensional base. $M_\infty = 2.41$.

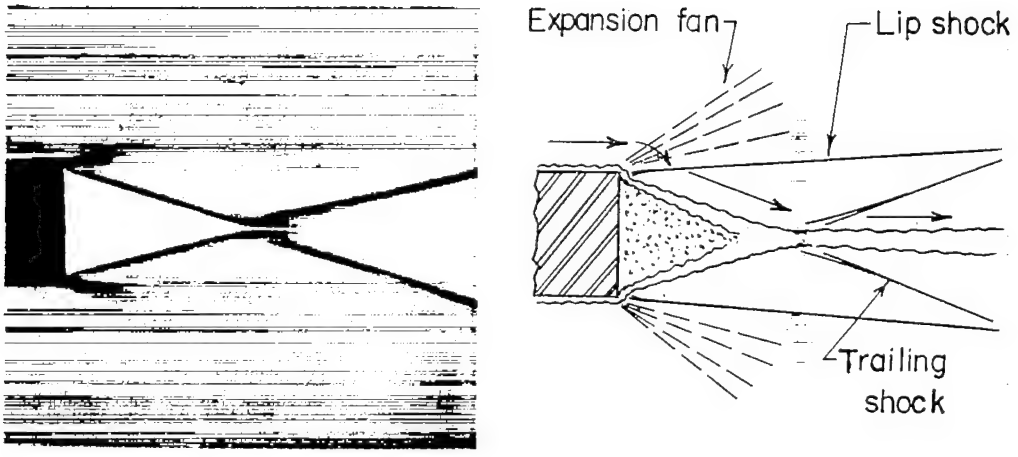


(a) Two-dimensional base.

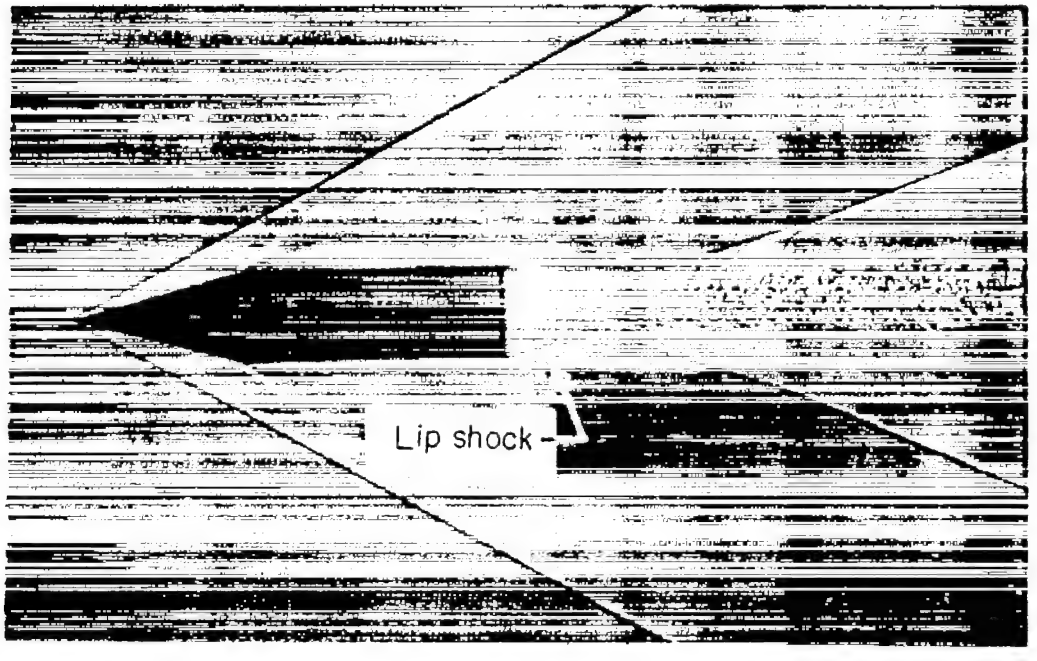


(b) Body of revolution.

NACA
L-77945

Figure 11.- The lip shock phenomena occurring at the base of bodies at supersonic speeds.

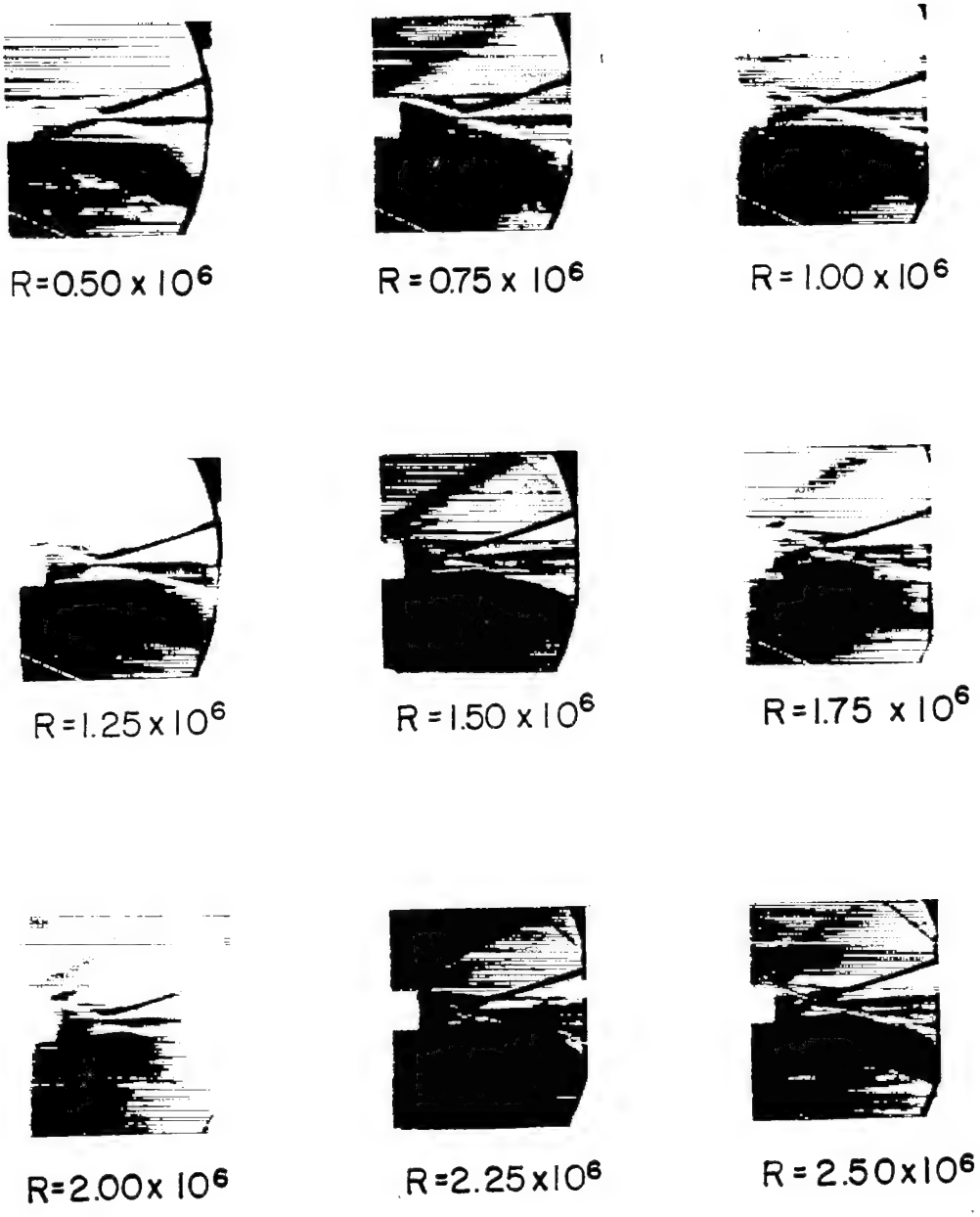


Figure 12.- Flow phenomena behind two-dimensional base showing relation between lip shocks and wake convergence with varying Reynolds number. $M_\infty = 2.41$; $\alpha = 0^\circ$.

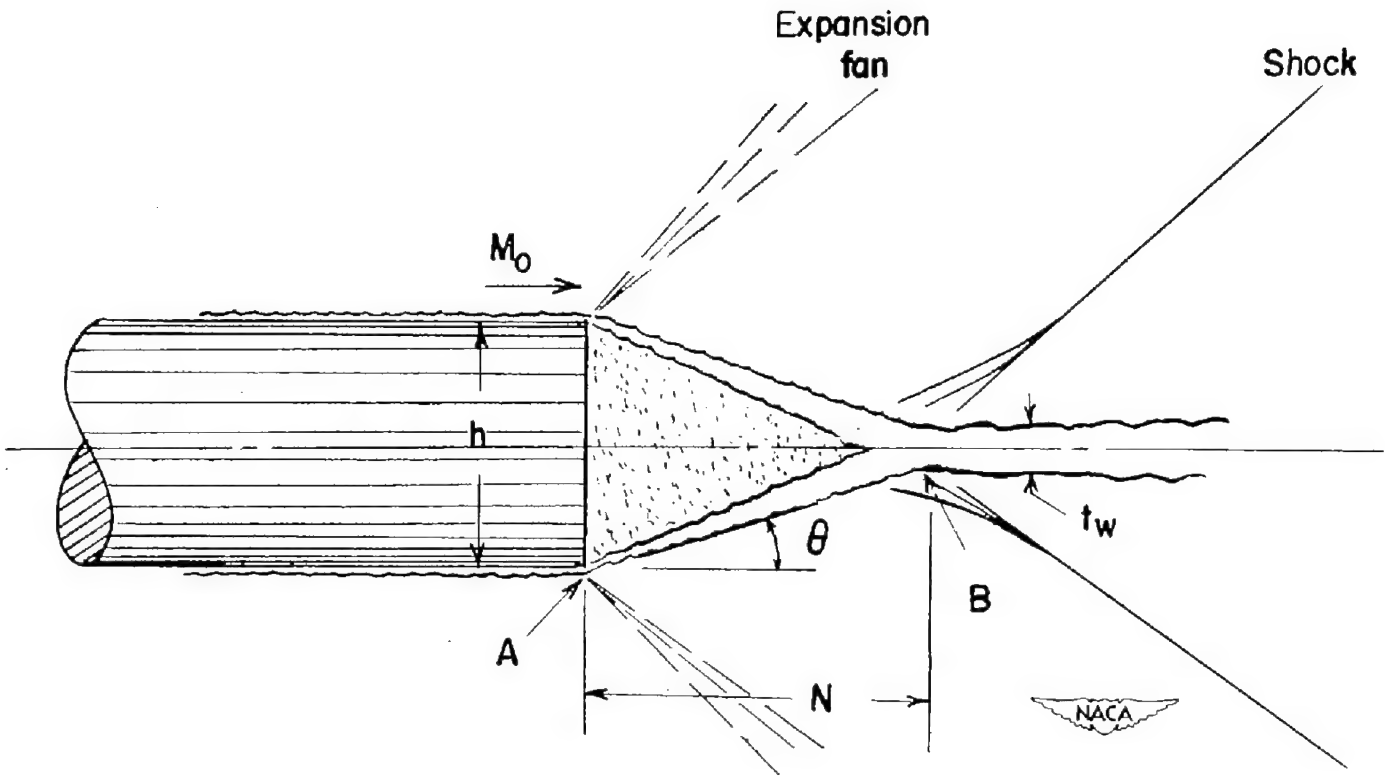


Figure 13.- Sketch of base phenomena for a body of revolution.

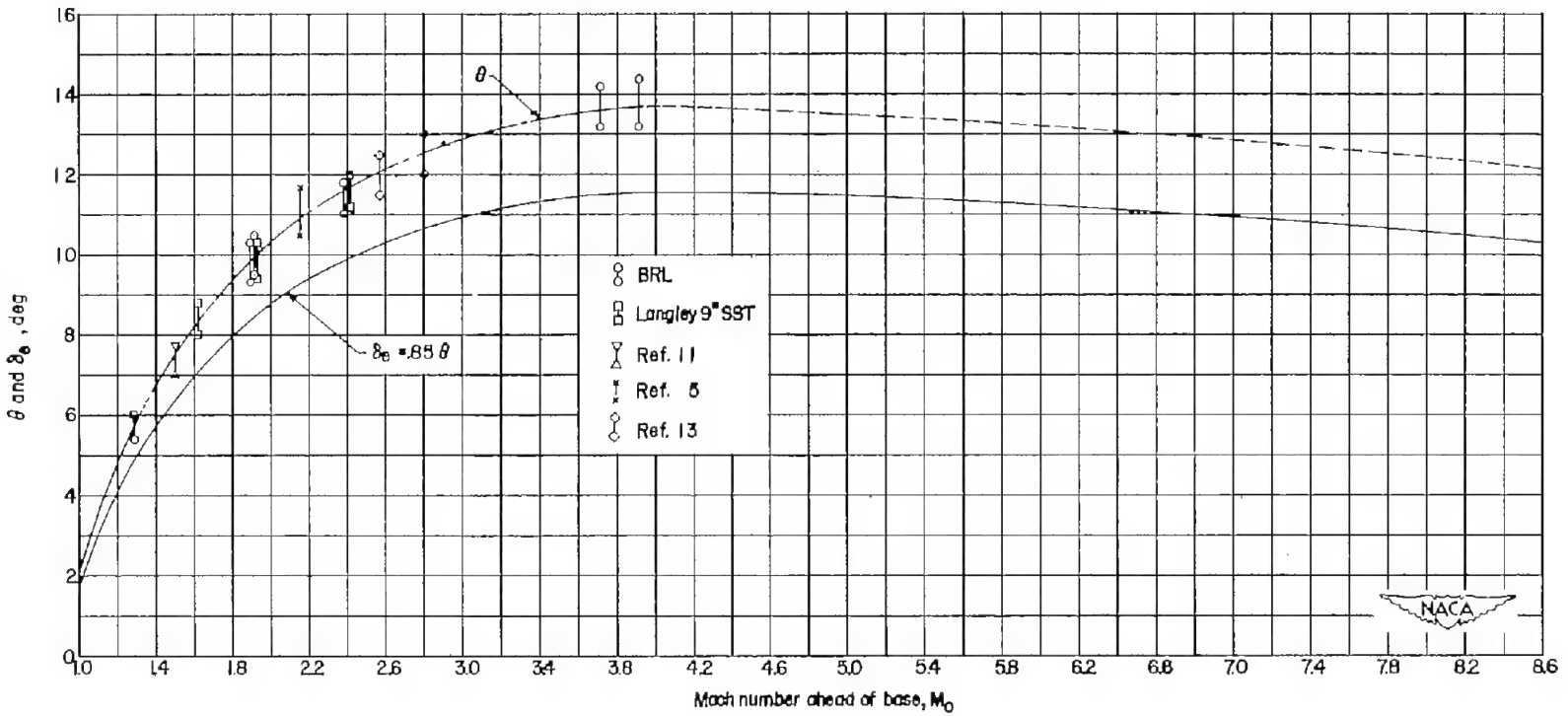


Figure 14.- Variation of wake convergence $\theta$ and effective two-dimensional convergence $\delta_e$ with Mach number ahead of base.

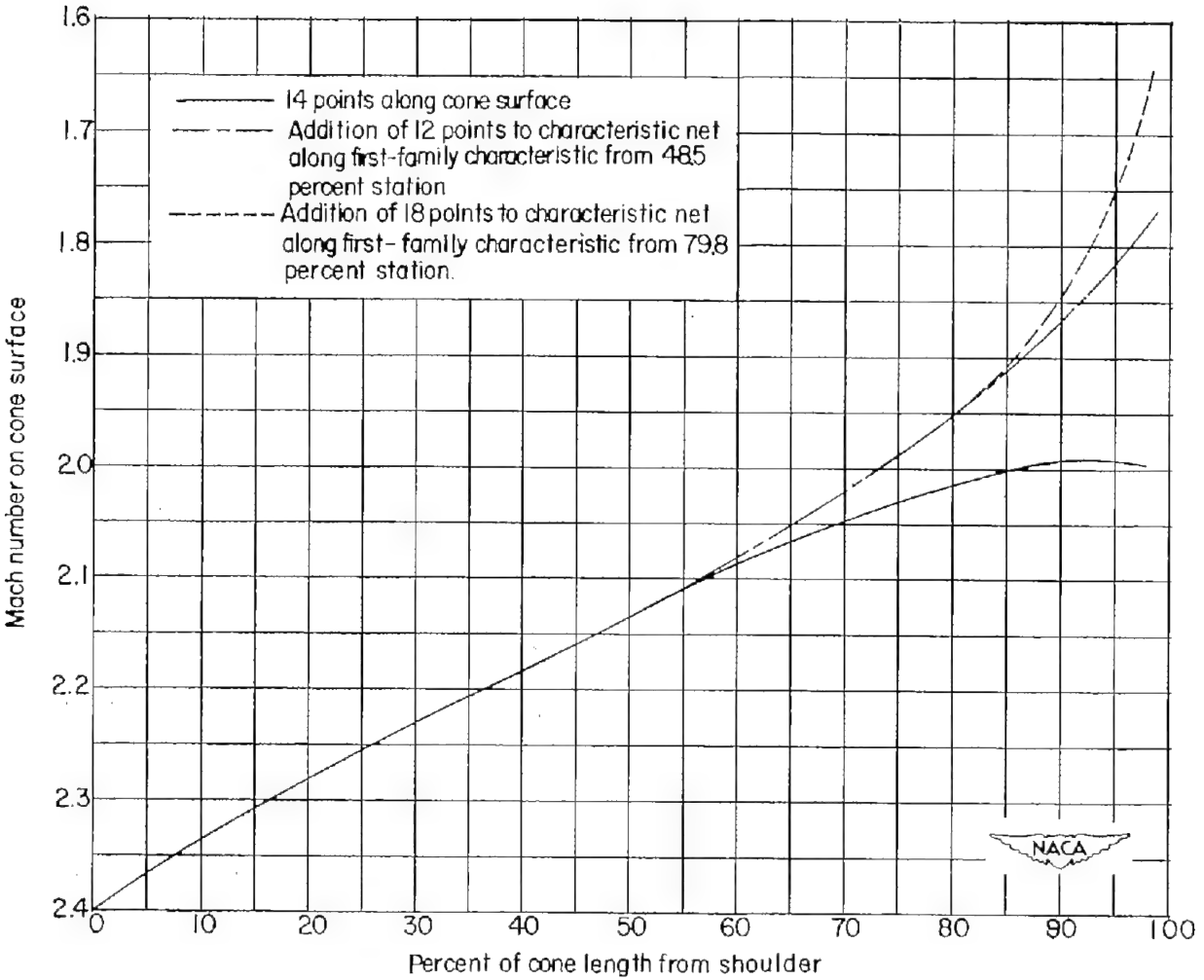


Figure 15.- Calculations by the method of characteristics of recompression over a 10.33° conical boattail for $M_o = 2.00$ showing effects of refinements to characteristic net.

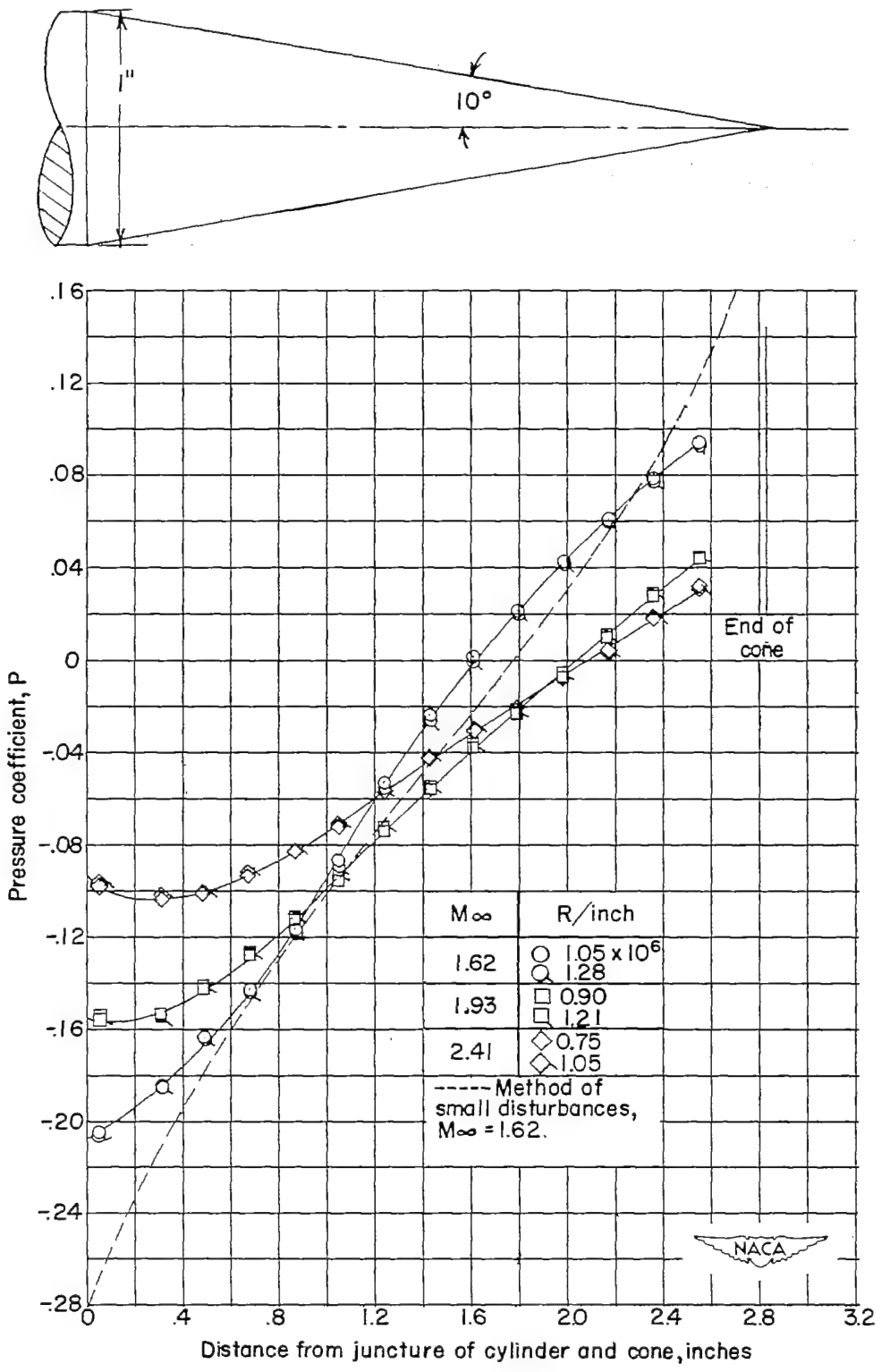


Figure 16.- Recompression over a 10° conical afterbody. $\alpha = 0^{\circ}$.

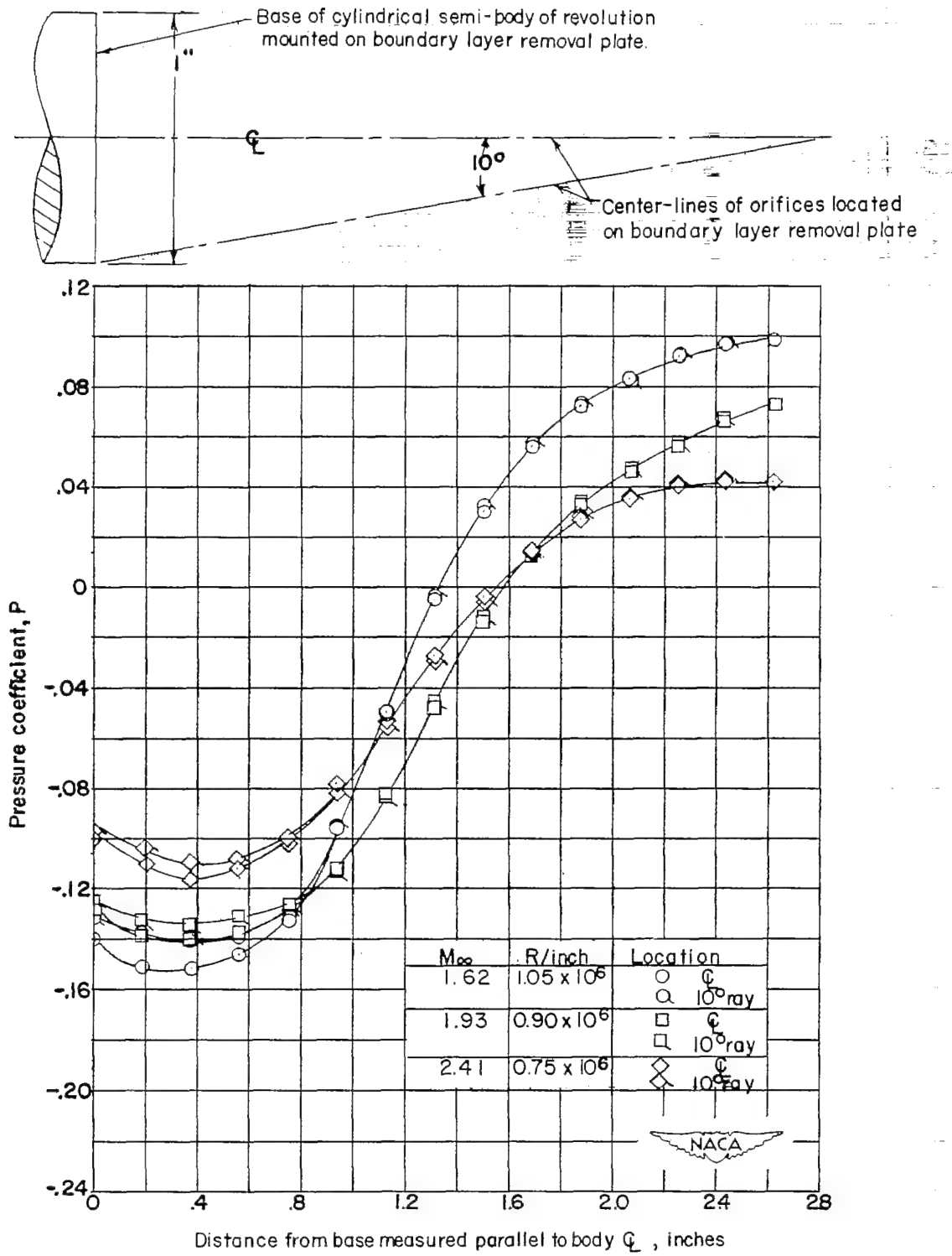


Figure 17.- Pressure variation within the wake behind the base of a cylindrical body. $\alpha = 0^{\circ}$.

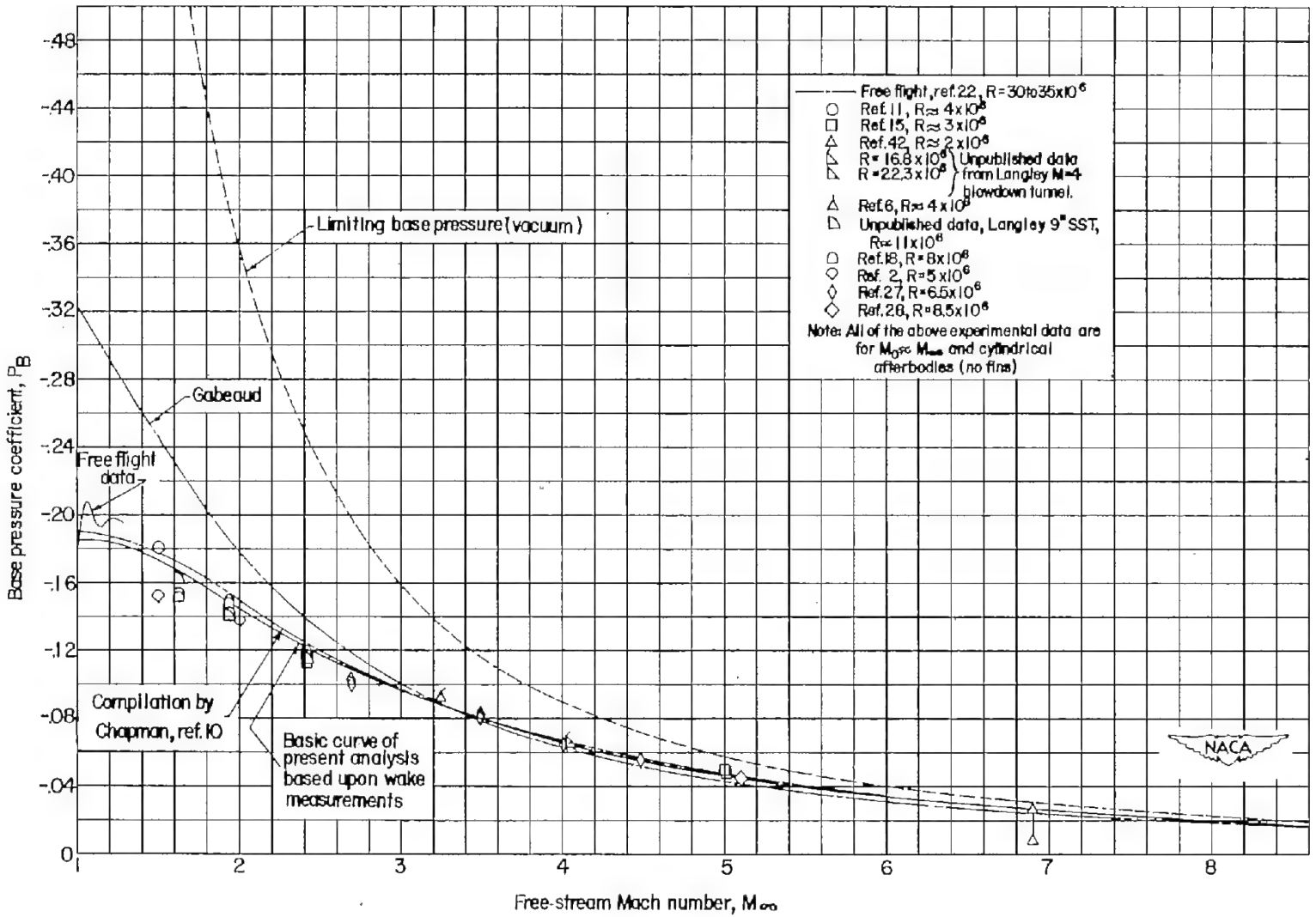


Figure 18.- Base pressure on bodies of revolution having cylindrical afterbodies (no fins).

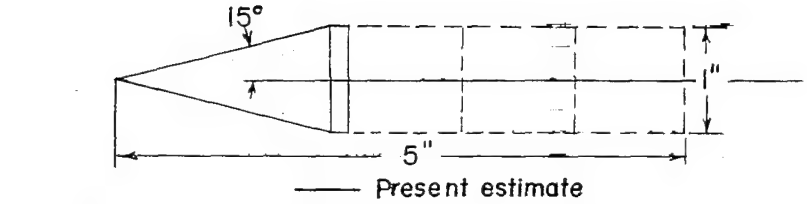


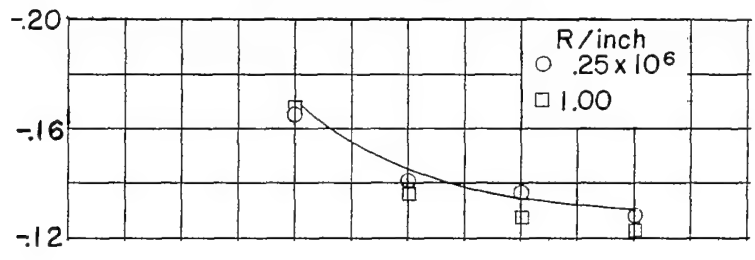


(a) $M_\infty = 2.41$.

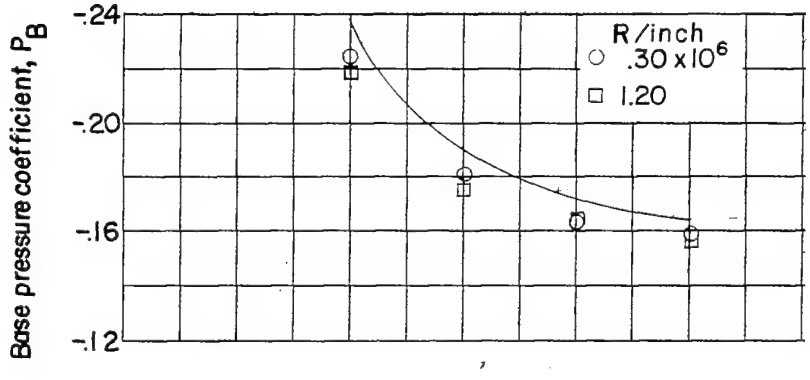


(b) $M_\infty = 1.93$.

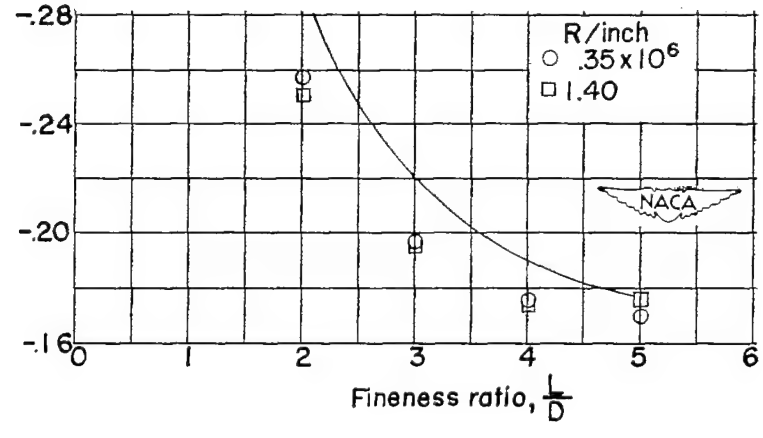


(c) $M_\infty = 1.62$.

Figure 19.- Effects of fineness ratio upon base pressure for cone-cylinder bodies.

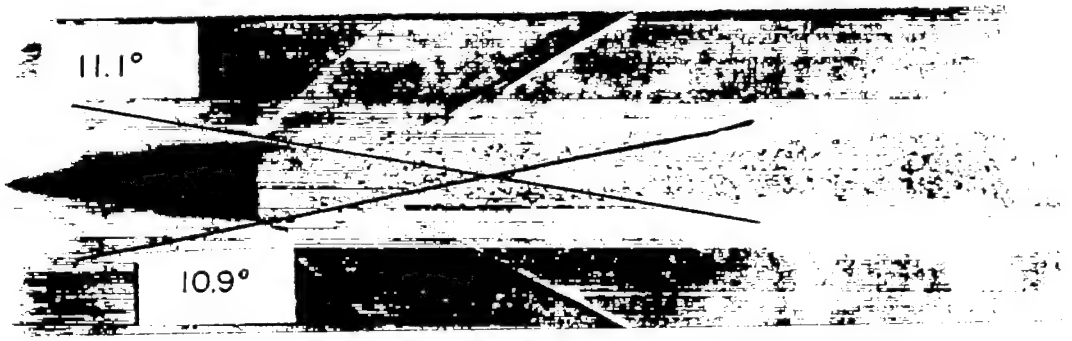


(a) $\frac{L}{D} = 2.84, M_0 \approx 2.03$


(b) $\frac{L}{D} = 5, M_0 \approx 1.86$

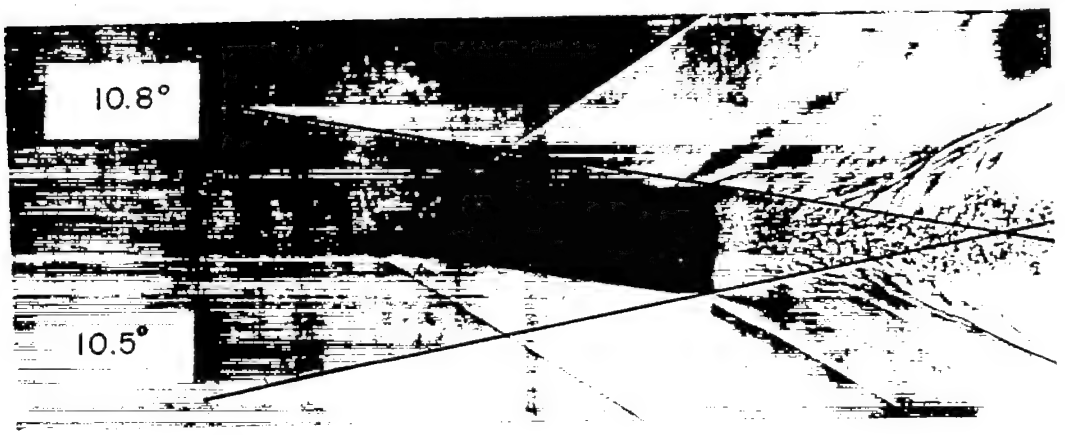


(c) $\frac{L}{D} = 3.14, M_0 \approx 1.99$

NACA
L-77947

Figure 20.- Effects of fineness ratio upon wake convergence for cone-cylinder bodies. $M_\infty = 1.84$. (Reproduction of shadowgraphs from tests conducted by Ballistic Research Laboratories.)

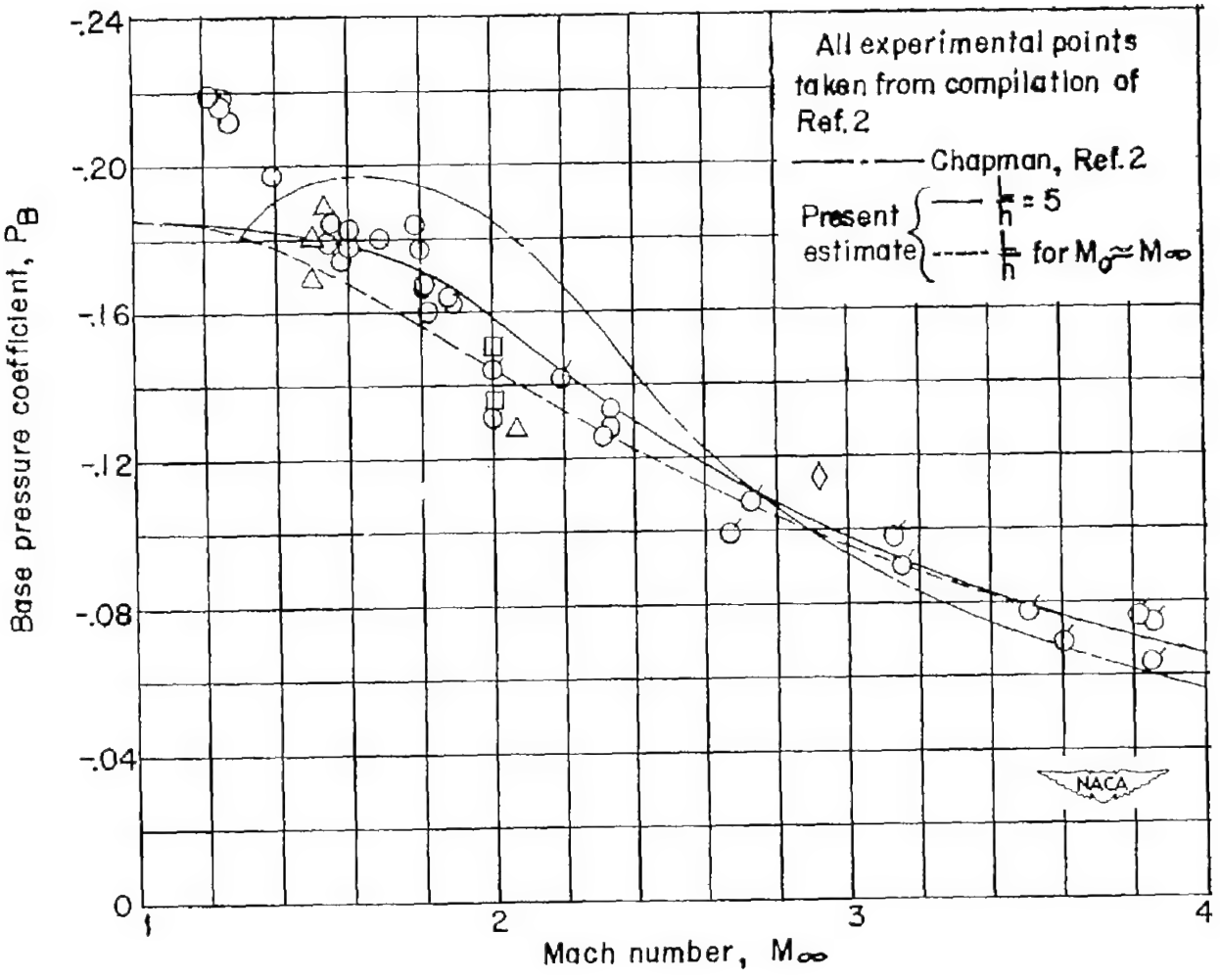


Figure 21.- Effects of Mach number upon the base pressure of 10° cone-cylinders of fineness ratio 5.

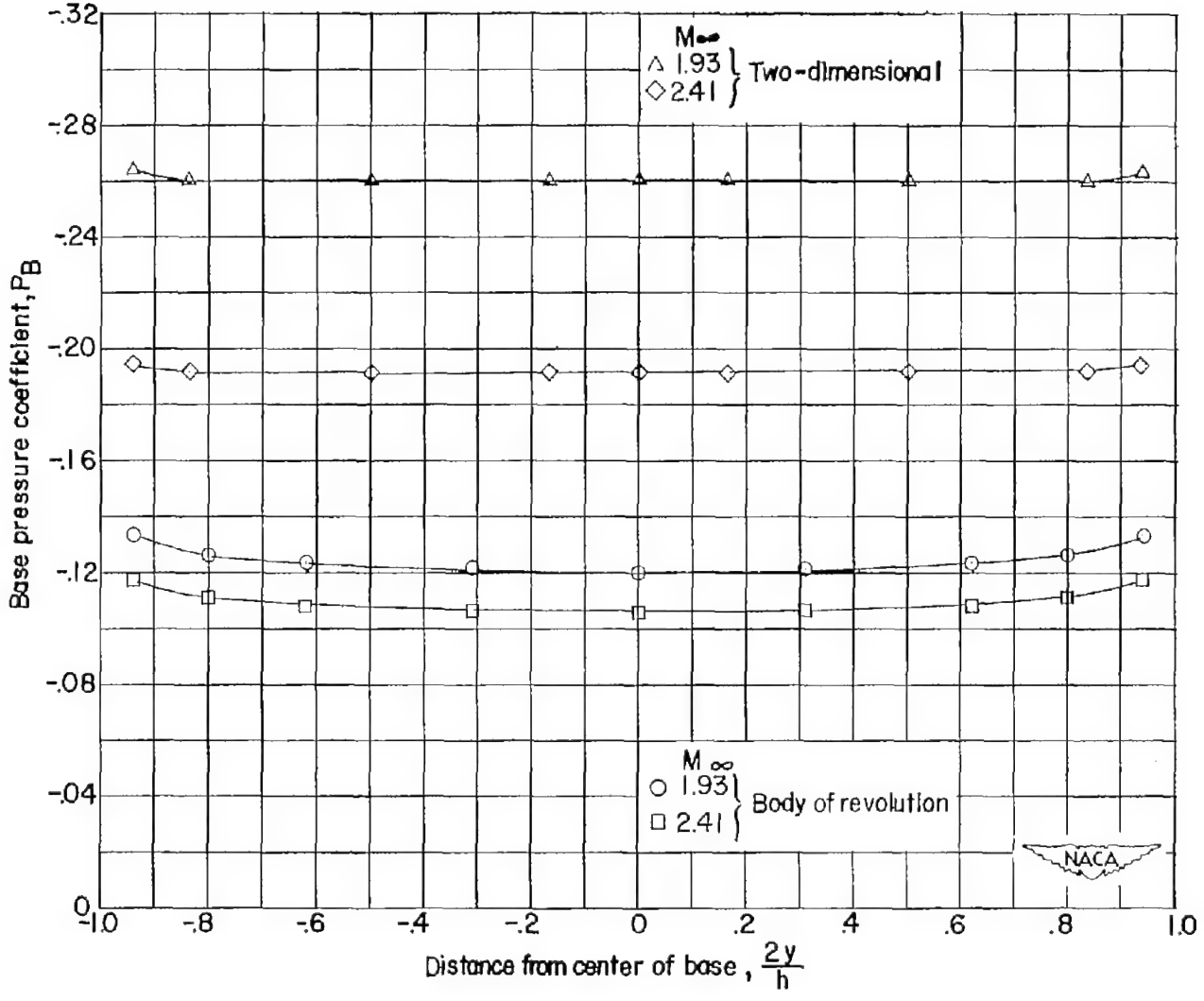


Figure 22.- Comparison of the pressure distributions across a two-dimensional base and the base of a body of revolution.

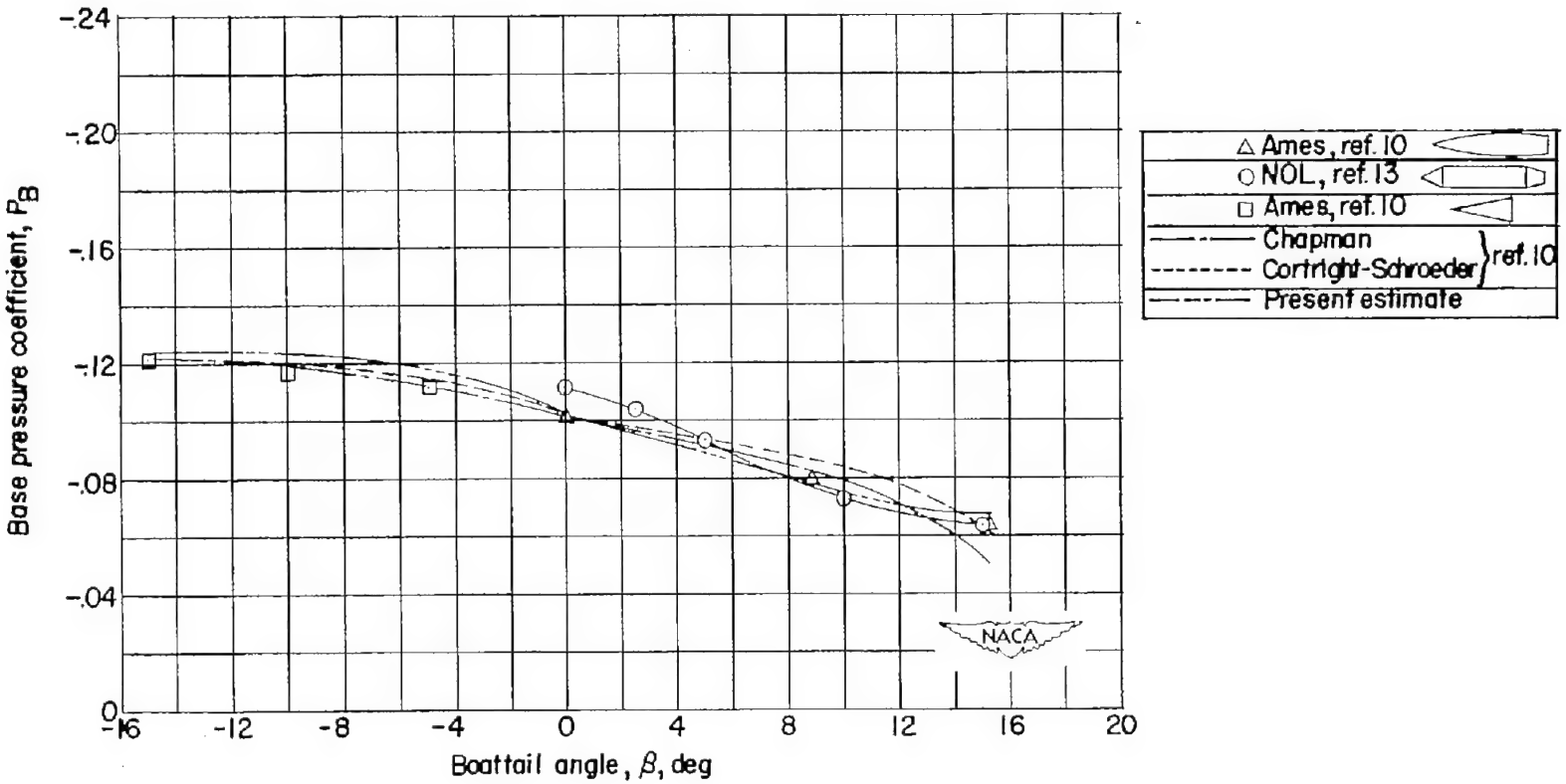


Figure 23.- Effects of boattailing upon base pressure for several configurations. $M_\infty \approx 2.9$.

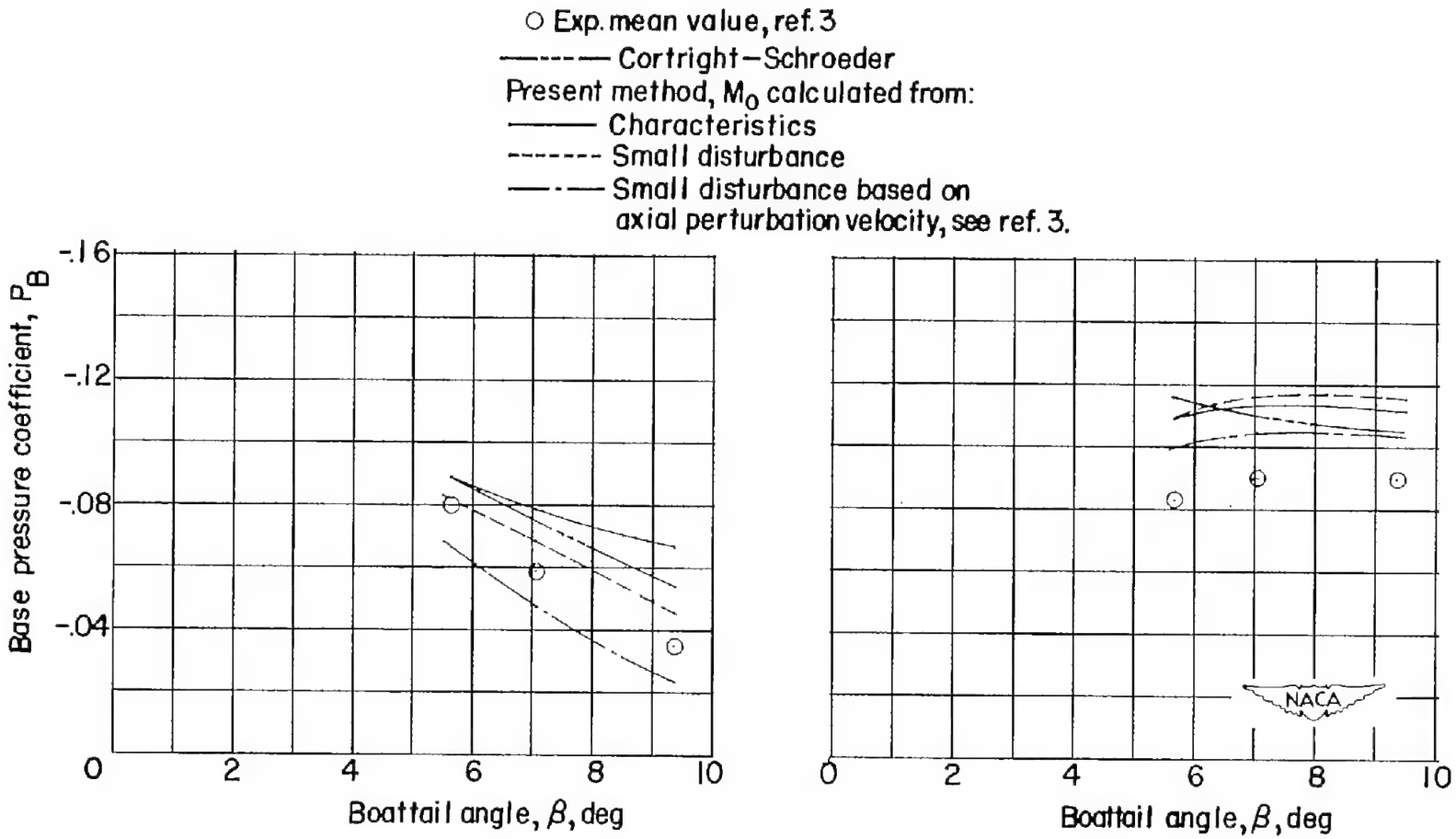


(a) $\frac{h}{D} = 0.506$.

(b) $\frac{h}{D} = 0.704$.

Figure 24.- Effects of conical boattailing and cut-off length upon base pressure. $M_\infty = 1.91$.

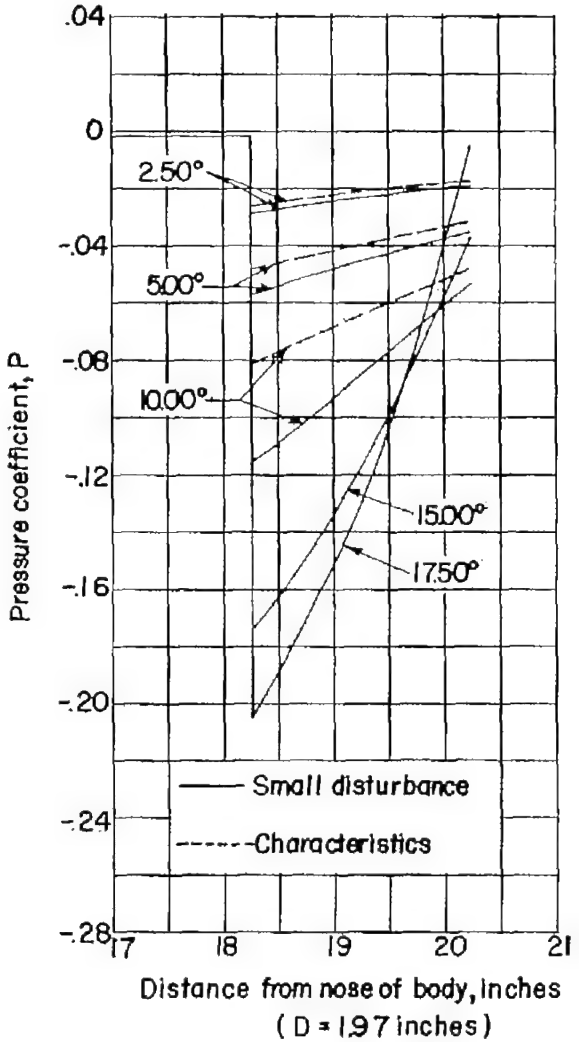


(a) Surface pressure on boattail.

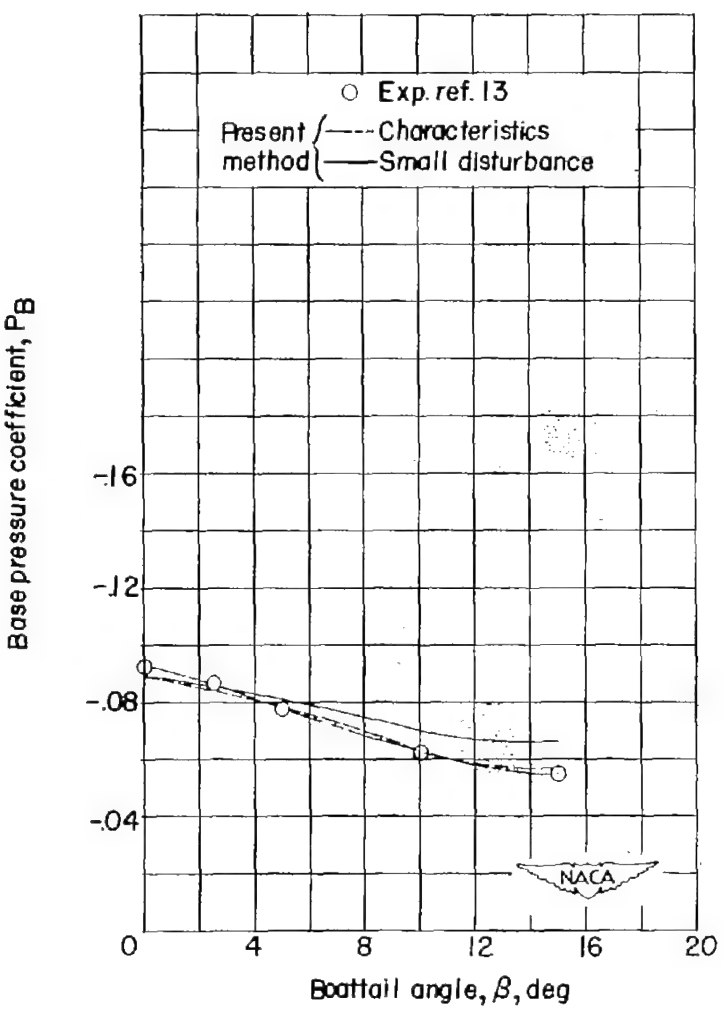


(b) Base pressure.

Figure 25.- Effects of conical boattailing upon base pressure. $M_\infty = 3.24$.

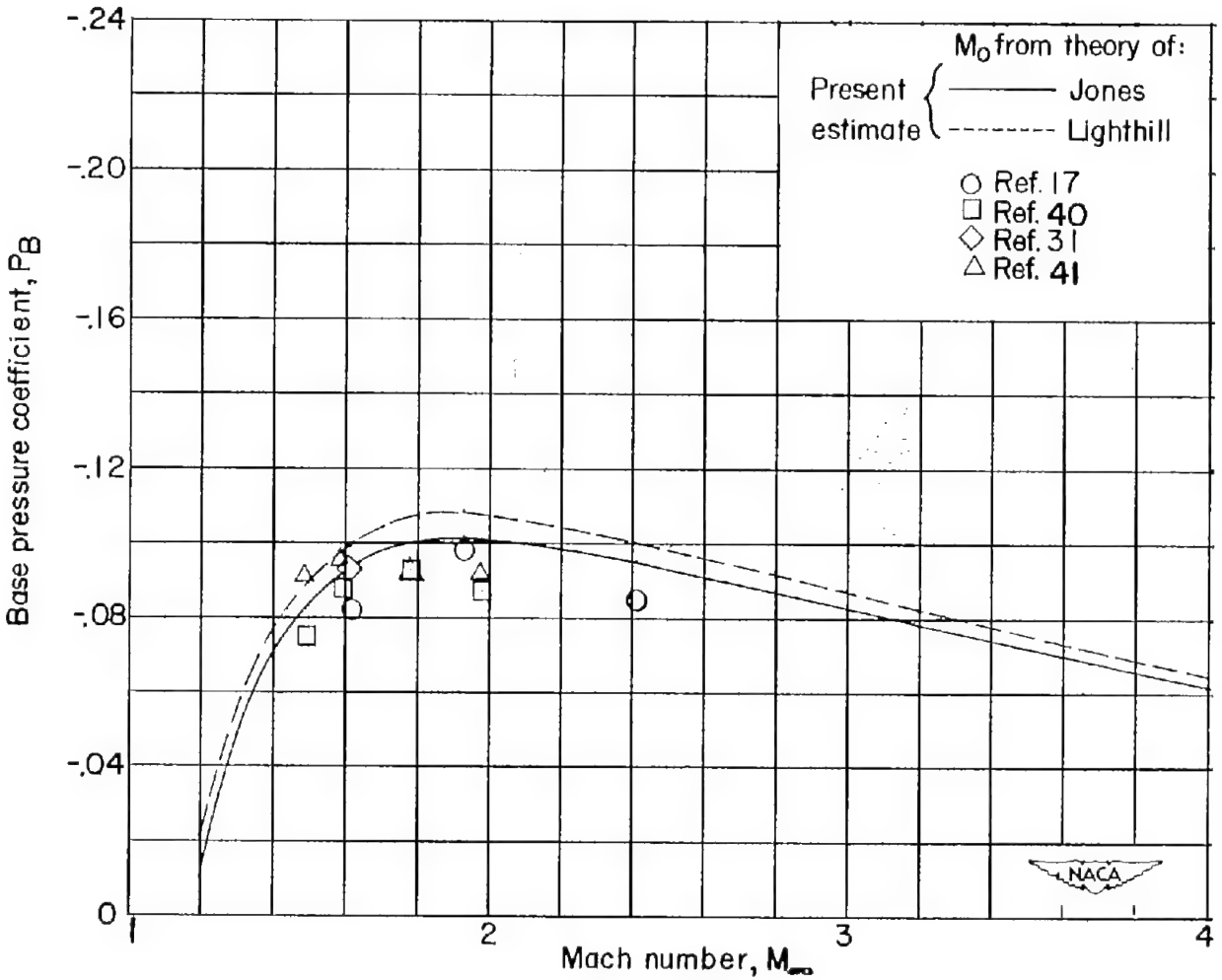


Figure 26.- Effects of Mach number upon the base pressure of the NACA RM-10 body (no fins).

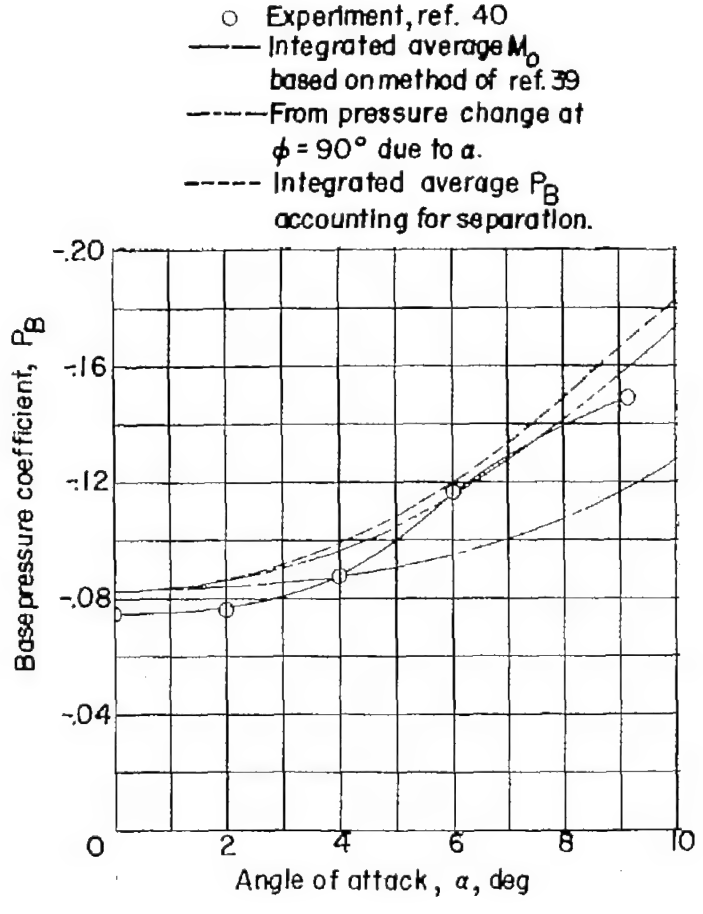


(a) Base pressure.

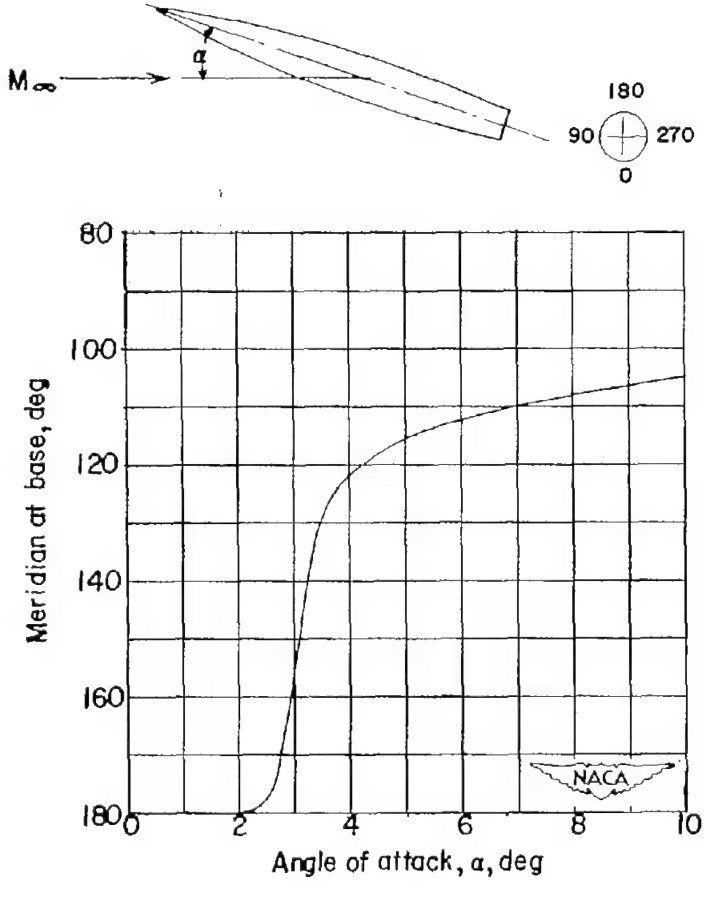


(b) Meridian for separation of flow at base.

Figure 27.- Effects of angle of attack upon the base pressure and the estimated value of the meridian for separation of flow at the base for the NACA RM-10 body (no fins), $M_\infty = 1.49$.

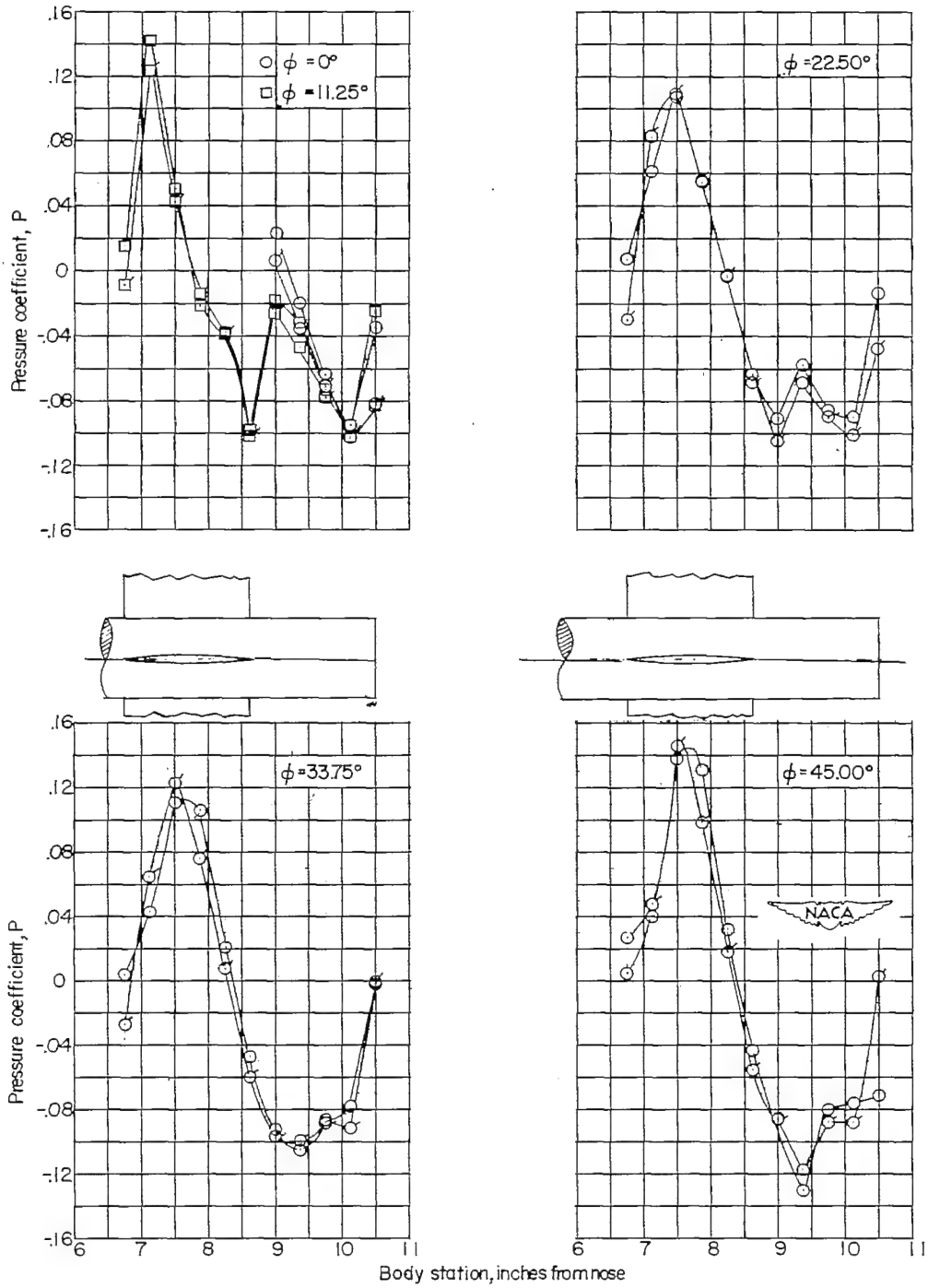


(a) $M_\infty = 1.93$; $R = 3.1 \times 10^6$ and $12.6 \times 10^6$ (flagged symbols).

Figure 28.- Fin effects upon body pressures. $\frac{t}{c} = 0.10$; $\frac{t}{D} = 0.15$.

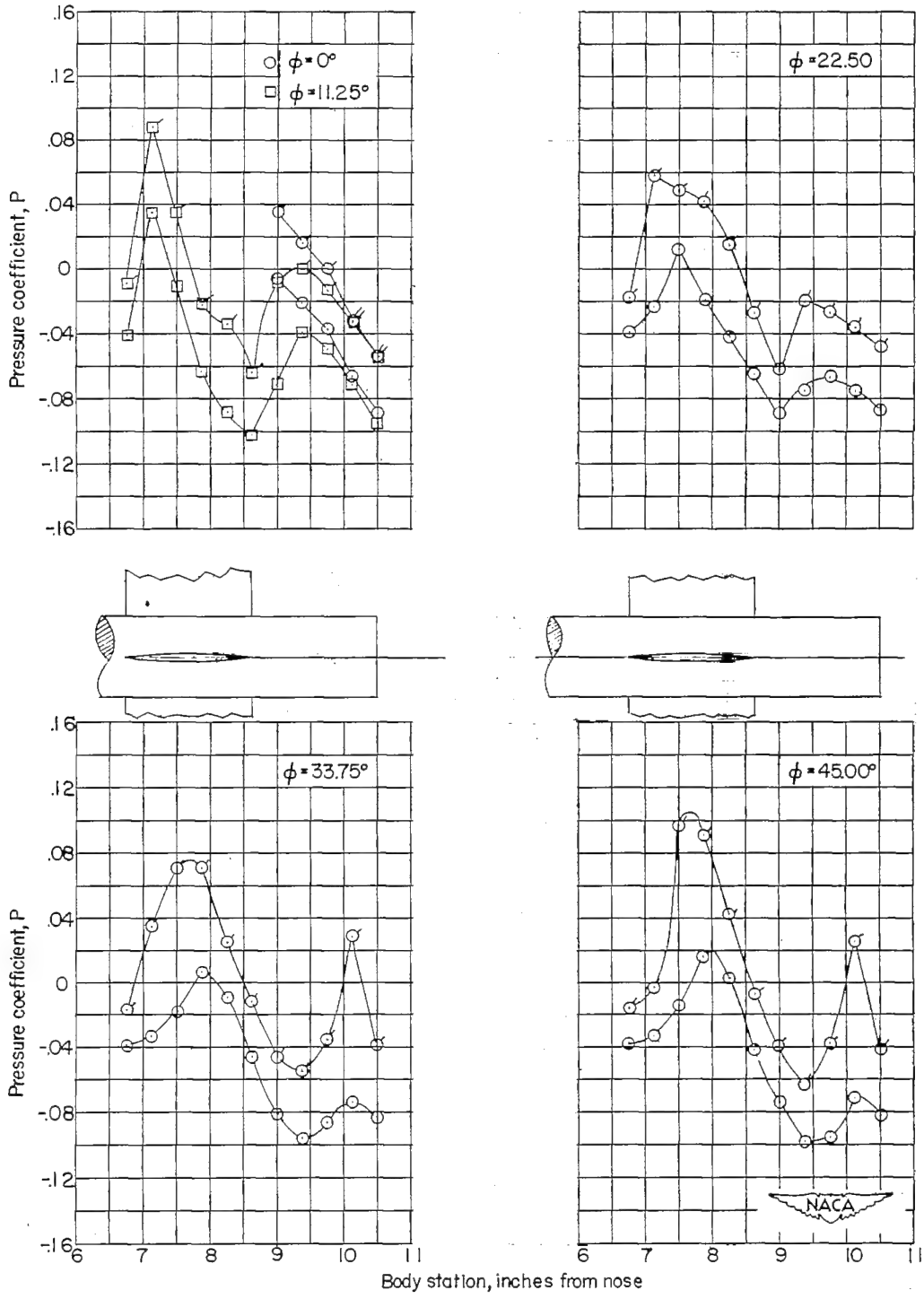


(b) $M_\infty = 2.41$; $R = 2.8 \times 10^6$ and $11.3 \times 10^6$ (flagged symbols).

Figure 28.- Concluded.

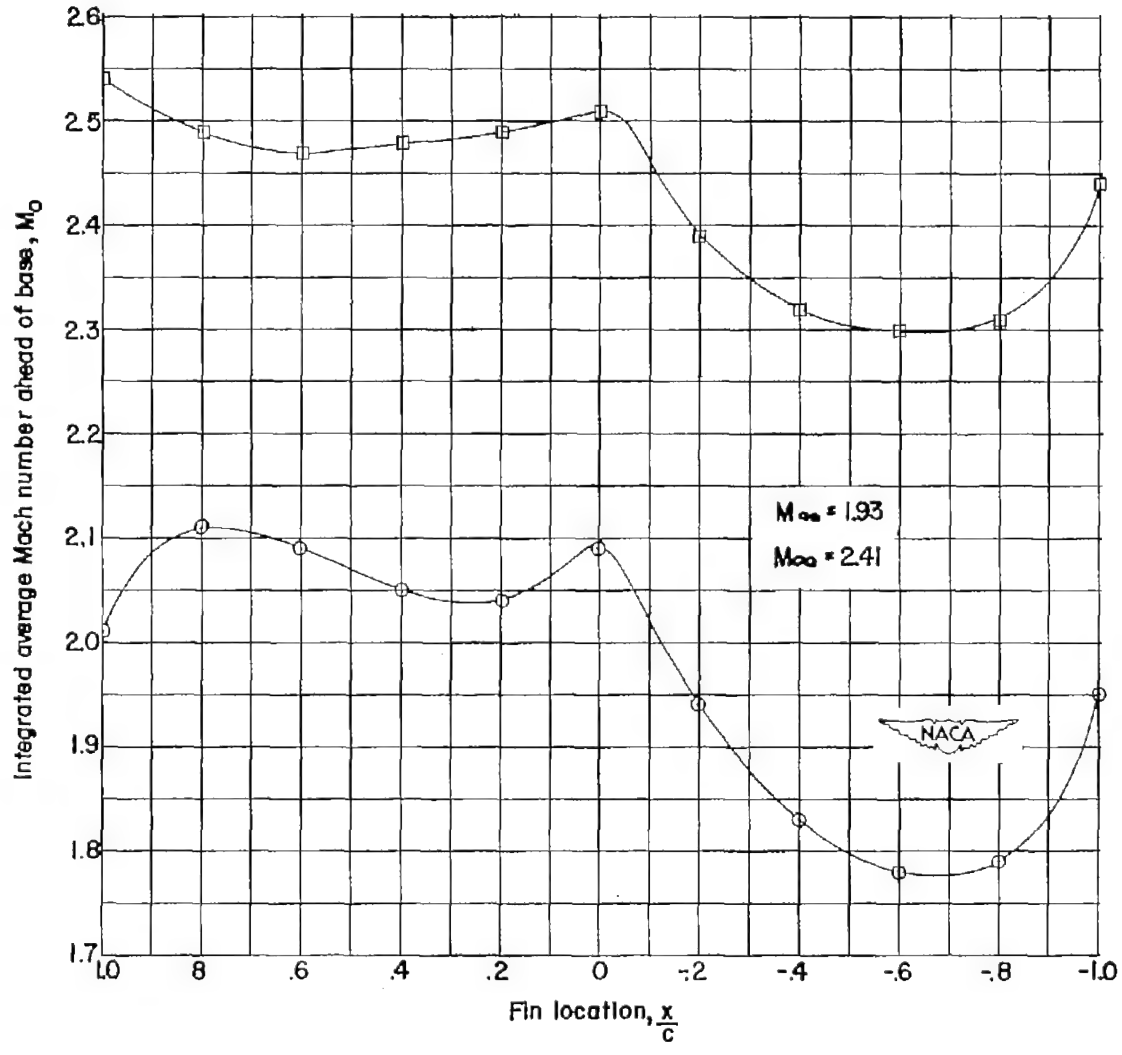


Figure 29.- Effect of fin location upon the integrated average Mach number ahead of the base, $M_0$.

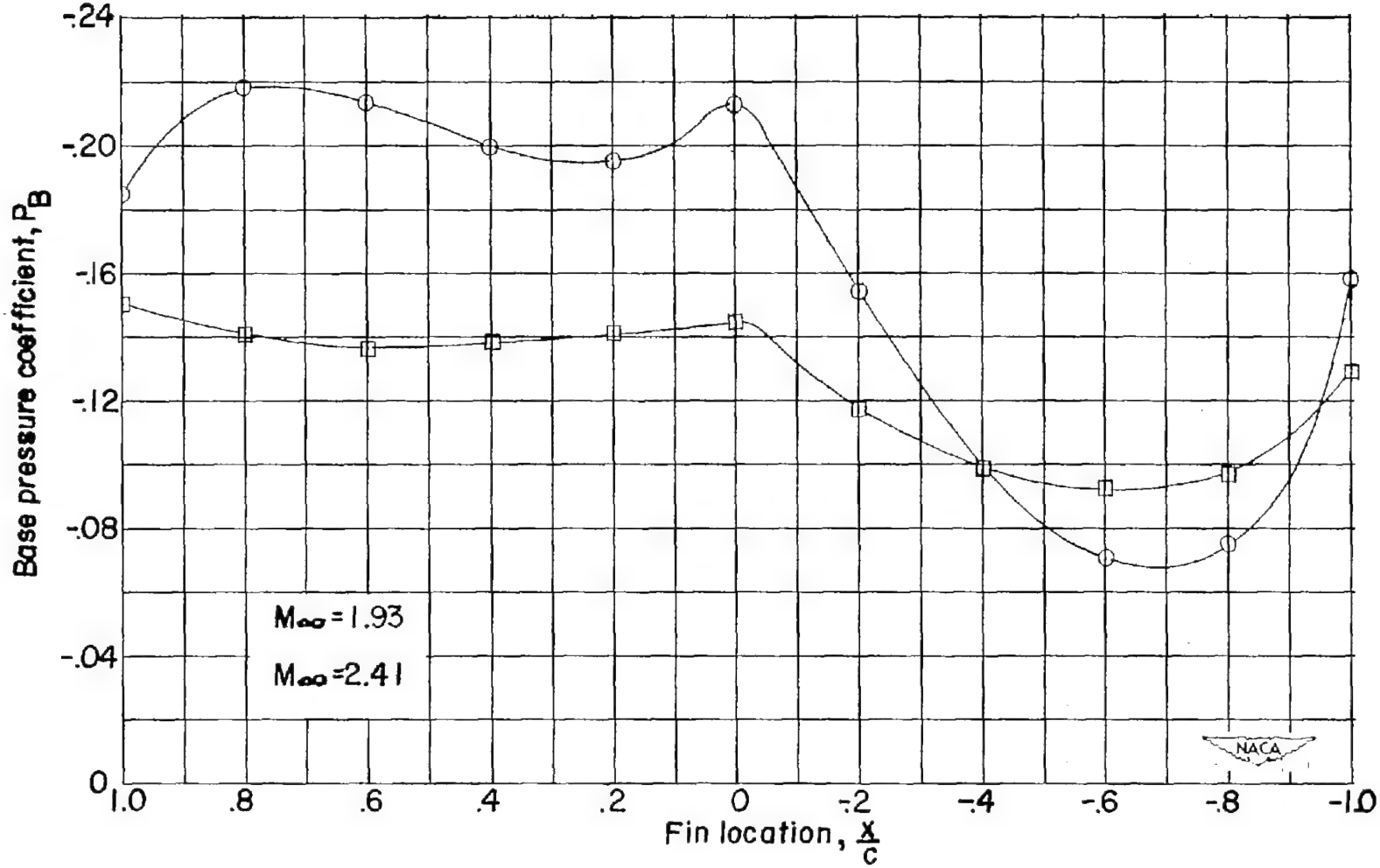


Figure 30.- Effect of fin location upon the base pressure calculated from the integrated average of value of $M_o$.

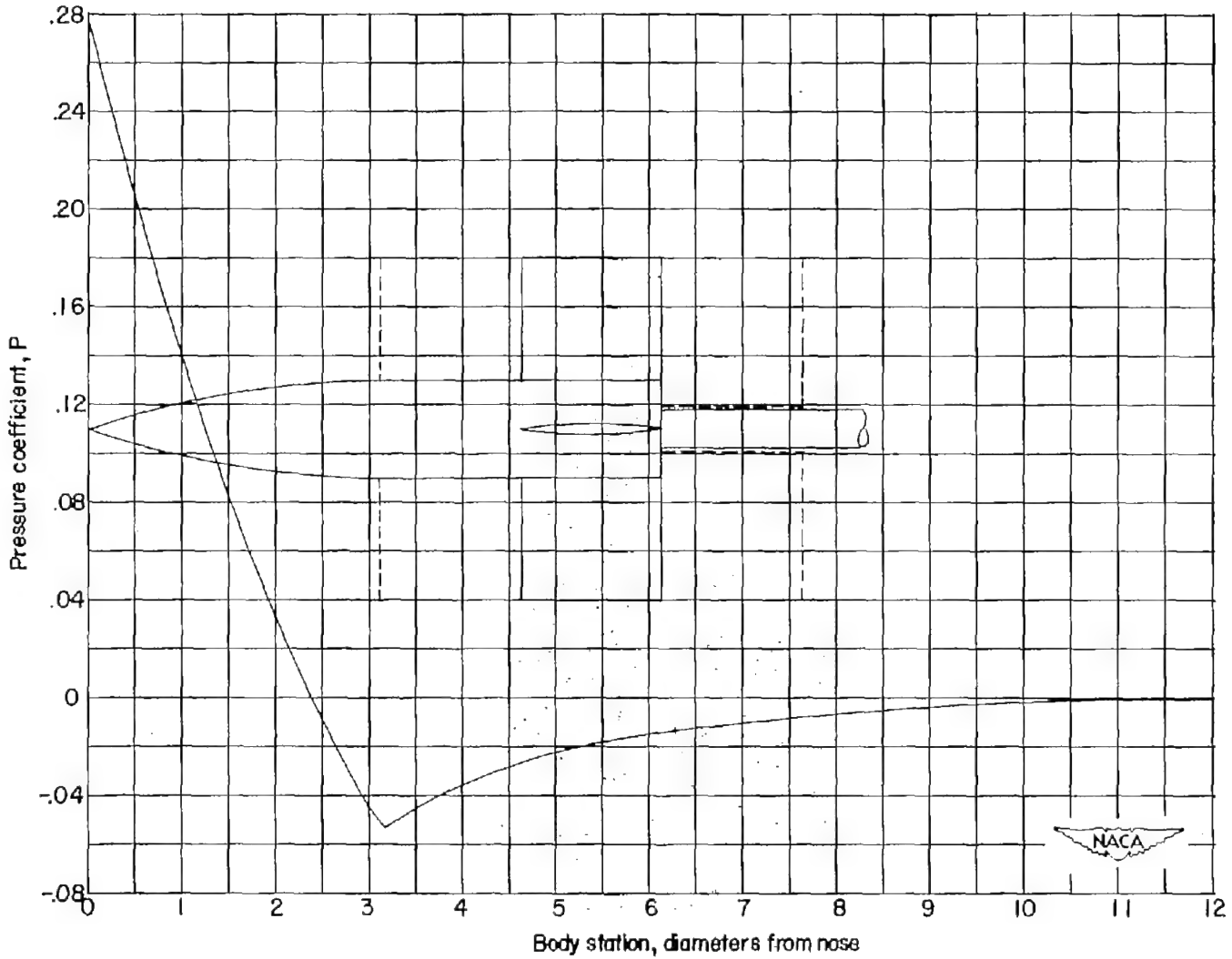


Figure 31.- Pressure distribution at $M_\infty = 2.00$ over the body alone for the configuration of reference 30 (10-caliber ogive with cylinder).

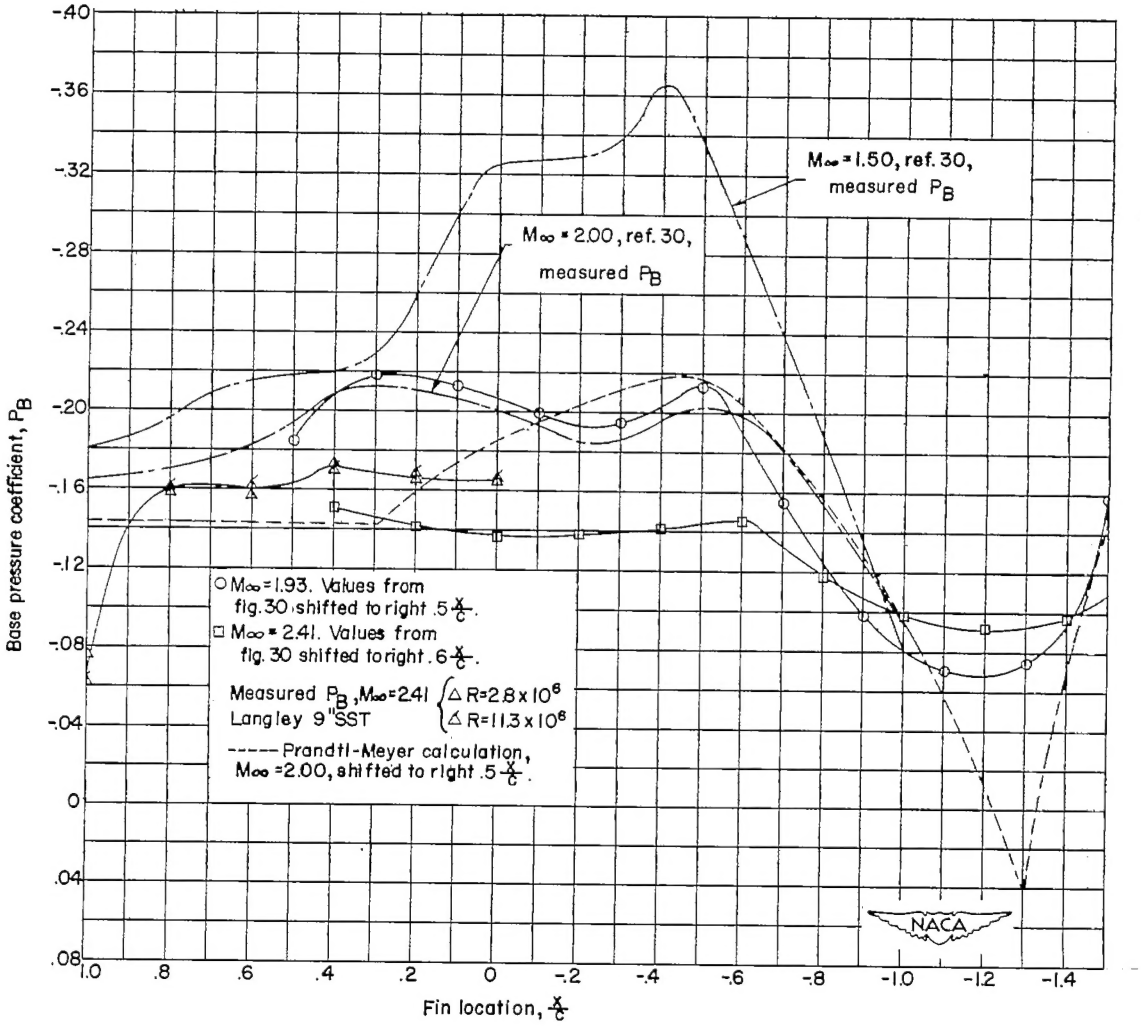


Figure 32.- Measurements and estimations of the effects of fin location upon base pressure at several Mach numbers.

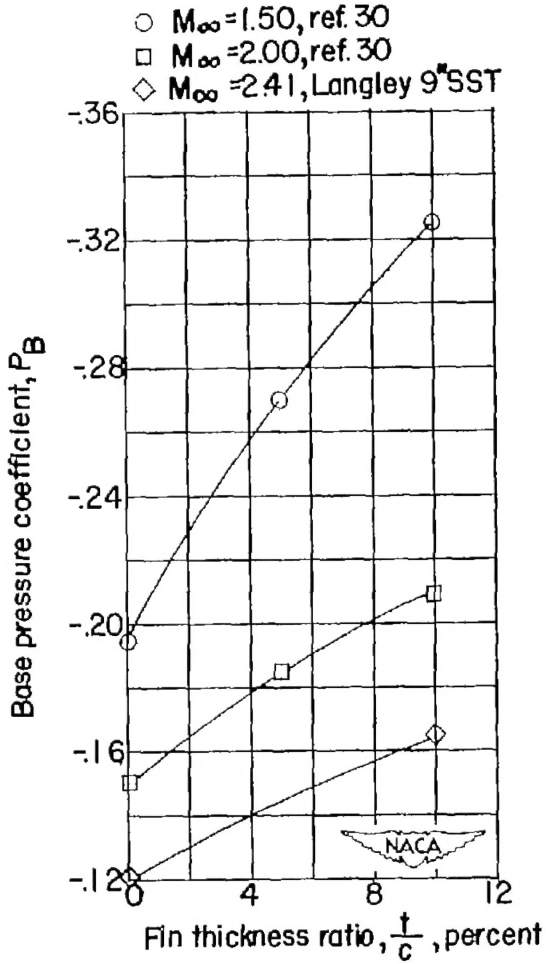


Figure 33.- Effects of fin thickness ratio of circular-arc fins upon the base pressure at $\frac{x}{c} = 0$ (zero sweepback).

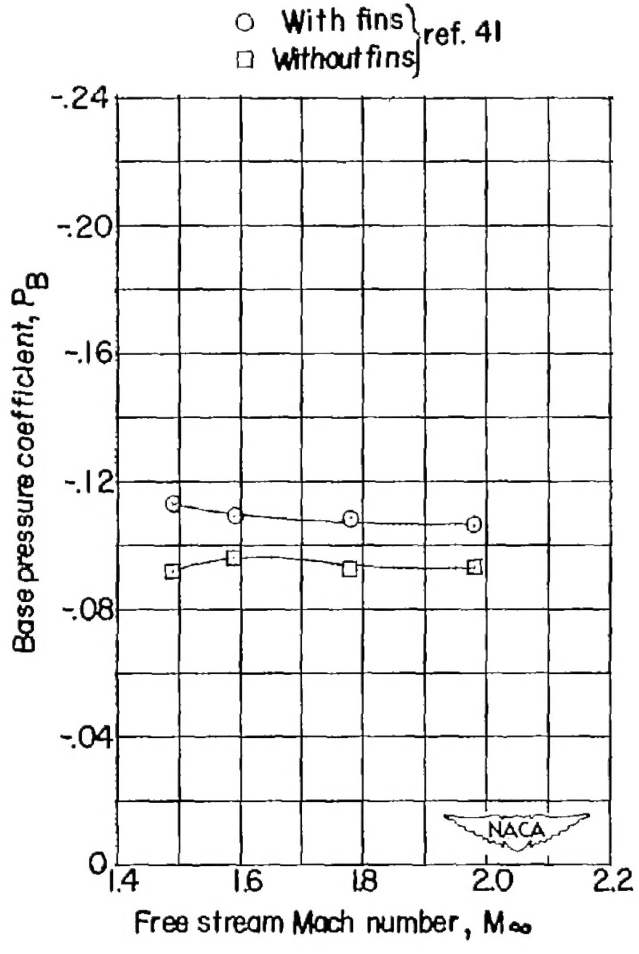


Figure 34.- Effects of fins upon the base pressure of the NACA RM-10 missile with varying Mach number. $\frac{t}{c} = 0.10$; 60° sweepback.

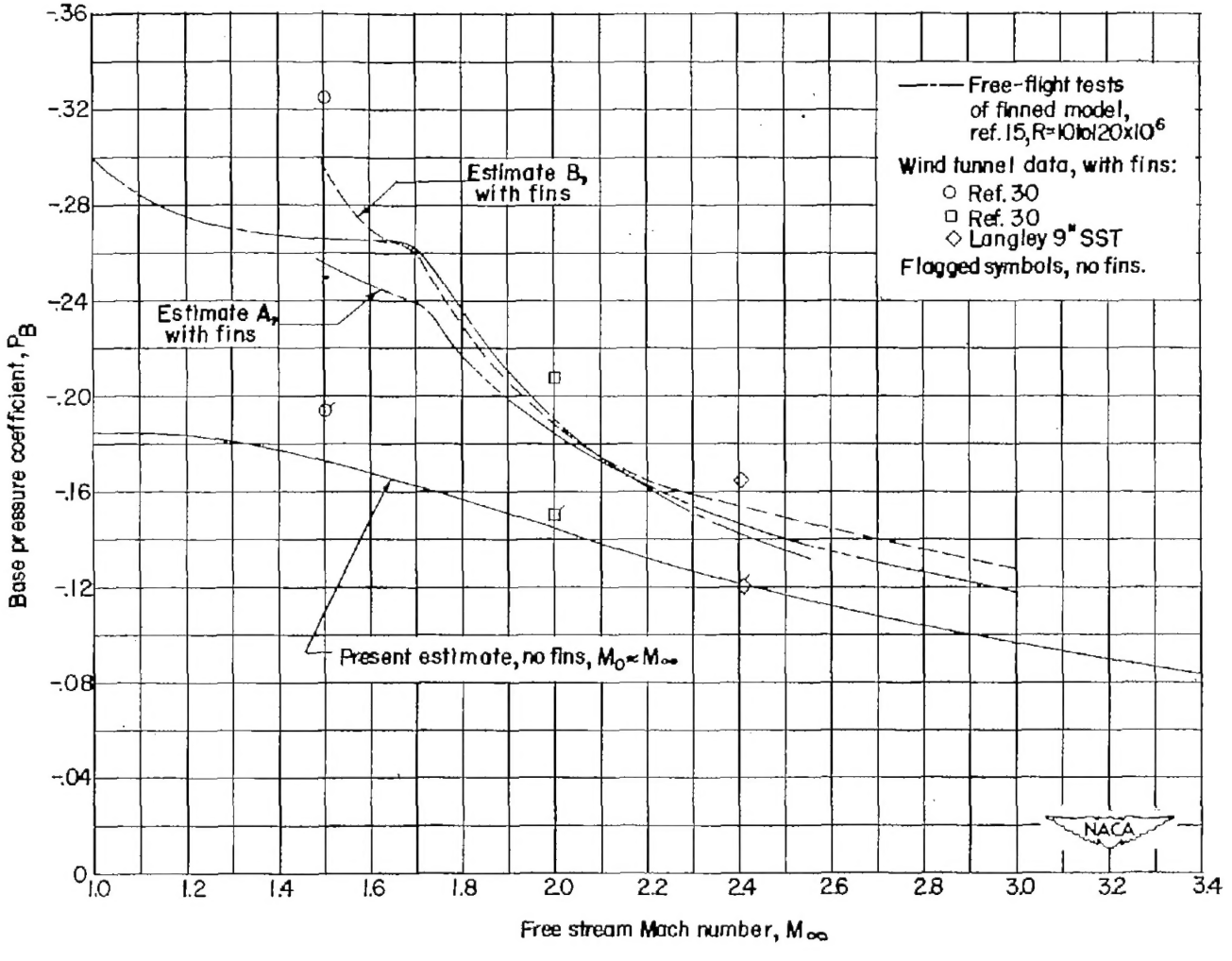


Figure 35.- Fin effects upon base pressure with varying Mach number. $\frac{t}{c} = 0.10$; $\frac{x}{c} = 0$; zero sweepback.

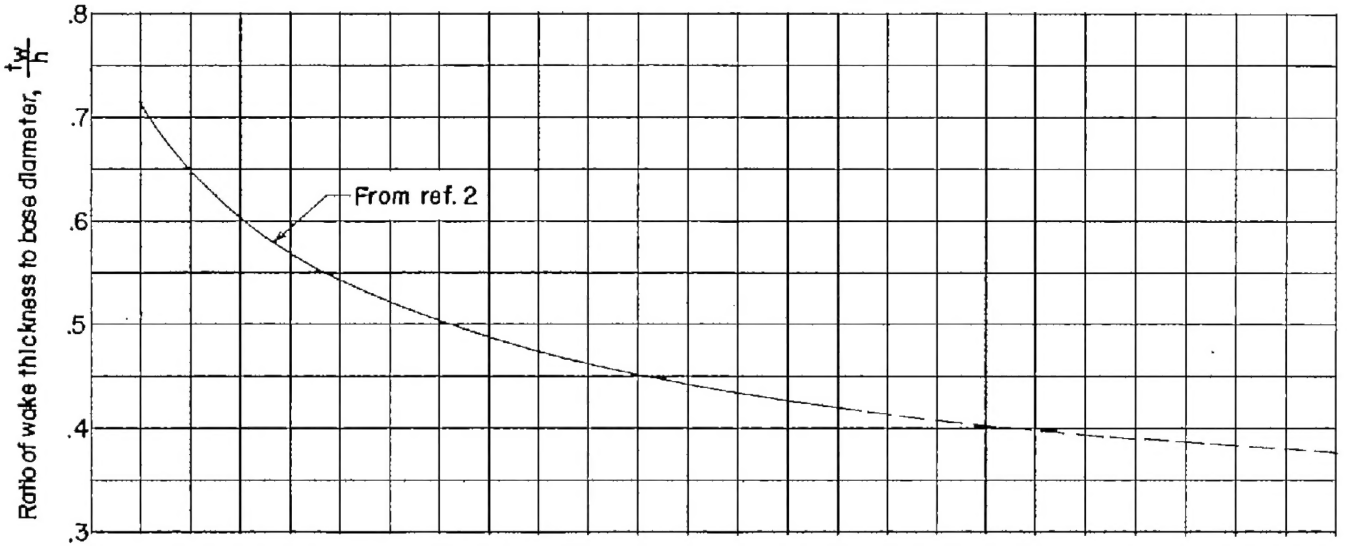


(a) Variation of wake thickness with Mach number.

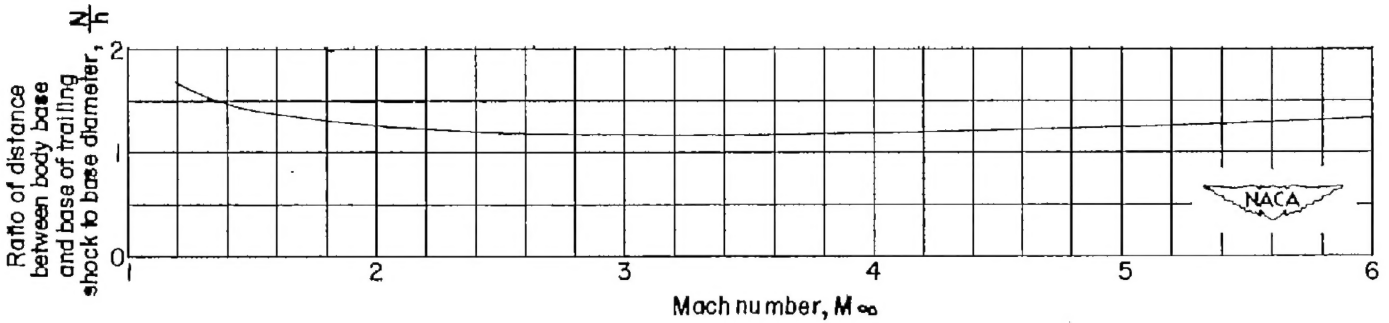


(b) Variation of location of base of trailing shock with Mach number.

Figure 36.- Approximations of wake thickness and location of base of trailing shock with varying Mach number.